ONLINE ECG SIGNAL ORTHOGONALIZATION BASED ON SINGULAR VALUE DECOMPOSITION

A THESIS

SUBMITTED TO THE DEPARTMENT OF ELECTRICAL AND ELECTRONICS ENGINEERING

AND THE INSTITUTE OF ENGINEERING AND SCIENCES

OF BILKENT UNIVERSITY

IN PARTIAL FULFILLMENT OF THE REQUIREMENTS

FOR THE DEGREE OF

MASTER OF SCIENCE

By

Burak Acar

September 1996

ONLINE ECG SIGNAL ORTHOGONALIZATION BASED ON SINGULAR VALUE DECOMPOSITION

A THESIS

SUBMITTED TO THE DEPARTMENT OF ELECTRICAL AND ELECTRONICS ENGINEERING

AND THE INSTITUTE OF ENGINEERING AND SCIENCES

OF BILKENT UNIVERSITY

IN PARTIAL FULFILLMENT OF THE REQUIREMENTS

FOR THE DEGREE OF

MASTER OF SCIENCE

By

Burak Acar

September 1996

I certify that I have read this thesis and that in my opinion it is fully adequate, in scope and in quality, as a thesis for the degree of Master of Science.

Prof. Dr. Hayrettin Köymen (Supervisor)

I certify that I have read this thesis and that in my opinion it is fully adequate, in scope and in quality, as a thesis for the degree of Master of Science.

Assist. Prof. Dr. Orhan Arıkan

I certify that I have read this thesis and that in my opinion it is fully adequate, in scope and in quality, as a thesis for the degree of Master of Science.

Prof. Dr. Ziya İder

Approved for the Institute of Engineering and Sciences:

Prof. Dr. Mehmet Baray
Director of Institute of Engineering and Sciences

ABSTRACT

ONLINE ECG SIGNAL ORTHOGONALIZATION BASED ON SINGULAR VALUE DECOMPOSITION

Burak Acar
M.S. in Electrical and Electronics Engineering
Supervisor: Prof. Dr. Hayrettin Köymen
September 1996

Electrocardiogram (ECG) is the measurement of potential differences occurring on the body due to the currents that flow on the heart during diastole and systole. Cardiac abnormalities cause uncommon current flows, leading to strange waveform morphologies in the recorded ECG. Since some abnormalities become visible in ECG only during activity, exercise ECG tests are conducted.

The sources of noise during an exercise test are electromyogram (EMG) due to increased muscle activity and baseline wander (BW) due to mechanical motion. Frequency band filtering, used to eliminate noise, is not an efficient method for filtering noise because usually frequency spectra of the interference and the ECG overlap. Rather, a fast morphological filter is required.

This thesis is focused on an online filtering approach which separates noise and ECG signals without changing the morphology. The redundancy present in standard 12 lead ECG records is made operational by a Singular Value Decomposition based orthogonalization of the input signals. ECG is represented in a minimum dimensional space whose orthogonal complement takes on noise. The signals in this low dimensional space are used to reconstruct the input signals without noise. Noise elimination also improves data compression. A comparative study of the ST analysis of original and reconstructed signals is presented at the end.

Keywords : Exercise ECG, Singular Value Decomposition (SVD), Online Orthogonalization, Online Filtering.

ÖZET

TEKİL DEĞER AYRIŞTIRILMASI KULLANILARAK EKG SİNYALLERİNİN GERÇEK ZAMANDA BİRBİRLERİNE DİK ALTUZAYLARA AYRIŞTIRILMASI

Burak Acar
Elektrik ve Elektronik Mühendisliği Bölümü Yüksek Lisans
Tez Yöneticisi: Prof. Dr. Hayrettin Köymen
Eylül 1996

Elektrokardiyogram (EKG), kalpten sistol ve diyastol sırasında yayılan elektrik akımlarının vücudun yüzeyinde oluşturduğu potansiyel farkların ölçümüdür. Kardiyolojik bozukluklar EKG'de normal olmayan morfolojilere neden olurlar. Bu anormalilerden bazıları sadece aktivite sırasında gözlenebildiği için Eforlu EKG Testi uygulanmaktadır.

Eforlu EKG Testi sırasında EKG'yi kirleten iki temel gürültü kaynağı vardır; artan kas aktivitesine bağlı olarak elektromiyogram (EMG) kaynaklı gürültü ve mekanik harekete bağlı olarak referans potansiyelindeki oynama. Gürültüyü temizlemek için kullanılan frekans filtreleme yeterli bir yöntem değildir çünkü gürültünün ve EKG'nin frekans bantları çakışabilir. Frekans filtreleme yerine hızlı bir morfolojik filtreye ihtiyaç vardır.

Bu tezin konusu, gürültüyü EKG sinyallerinin morfolojisini bozmadan ayıran ve gerçek zamanda çalışan bir filtreleme yöntemidir. Bu amaçla standard 12 kanal EKG sinyallerindeki fazla bilgiden, bir başka deyişle kanallar arasındaki korelasyondan yararlanılmıştır. Bu fazla bilgi Tekil Değer Ayrıştırması yapan bir dikleştirme algoritması ile işe yarar kılınmıştır. Sonuçta EKG minimum boyutlu bir uzayda ifade edilmiş, bu uzaya dik olan uzayda ise gürültü kalmıştır. EKG'nin bulunduğu altuzaydaki sinyaller kullanılarak orijinal EKG derivasyonları gürültüsüz bir şekilde geri üretilmiştir. Gürültünün azaltılması EKG sinyallerinin sıkıştırılma kapasitesini de arttırmıştır. Orijinal sinyaller ile gürültüsüz olarak geri üretilen sinyaller üzerinden ST analizi yapılmış ve sonuçlar karşılaştırılmıtır.

Anahtar Kelimeler : Eforlu EKG, Tekil Değer Ayrıştırması, Gercek Zamanda Dikleştirme, Gercek Zamanda Filtreleme, Morfolojik filtre.

ACKNOWLEDGMENTS

I would like to express my sincere gratitude to Dr. Hayrettin Köymen for his supervision, guidance, suggestions, encouragement through the development of this thesis and his suggestions prior my presentation at Computers In Cardiology'96.

I would like to thank to Dr. Orhan Arıkan and Dr. Ziya İder for reading the manuscript and commenting on the thesis.

I am indebted to Kürşad Tüzer and Kiarash Farhood from Kardiosis Ltd. Co. for their assistance in data acquisition and analysis of the results and to Kerem Çağlar for his partnership. I would also like to thank to Savaş Dayanık for his help in statistical analysis of the results.

Special thanks are due to Dr. Orhan Arıkan and Dr. İrşadi Aksun for their suggestions and logistic support. I would like to express my appreciation to Umut Ersoy, Dr. Orhan Aytür, Burak Erdoğan, Kahraman G. Köprülü, Ayhan Bozkurt and to all of my friends in the department, whose names would make a very long list, for their continuous support through the development of this thesis. Finally, I would like to thank to my parents, brother and my grandmother, whose understanding made this study possible.

TABLE OF CONTENTS

LIST OF FIGURES

Chapter 1

INTRODUCTION

This thesis is focused on a new method of eliminating noise in *electrocardiogram* (ECG) signals acquired during stress test, based on an online orthogonalization algorithm.

ECG is the recorded electrical potentials generated by the heart during a cardiac cycle. An electrical impulse passes through the tissues causing small amount of electrical currents spreading all the way to the surface of the body. These currents generate the electrical potentials recorded in ECG. *Exercise (Stress) Test* is recording ECG, while the body is in action, for example while the patient runs on a treadmill. Figure 1.1 shows the location of the ECG recording leads on the body.

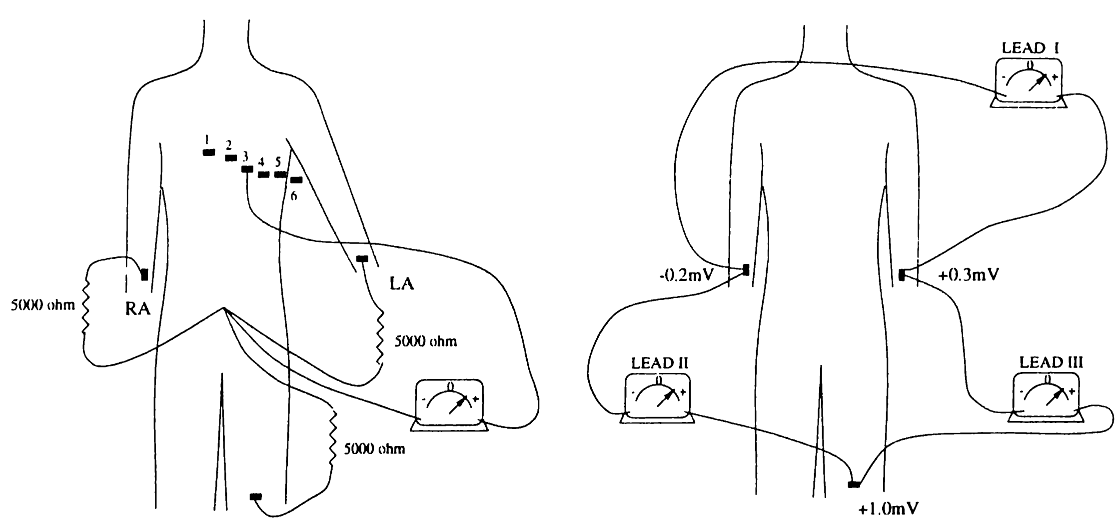

Figure 1.1: Standard leads used in ECG recording

The normal ECG is composed of a P wave, a QRS complex and a T wave.

QRS complex is actually three separate waves, the Q, R and S waves. All of them is caused by passage of the cardiac impulse through the ventricles. Figures 1.2 and 1.3 show typical heart beats recorded from standard channels.

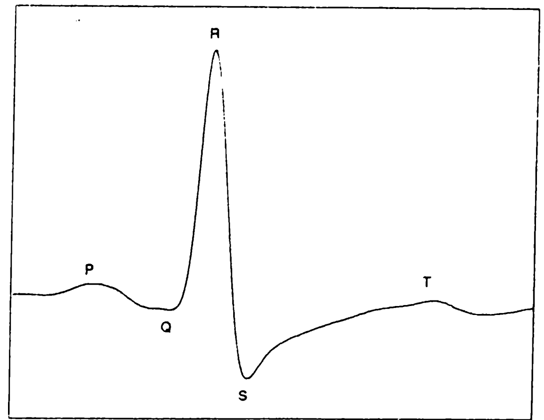

Figure 1.2: Typical heart beat

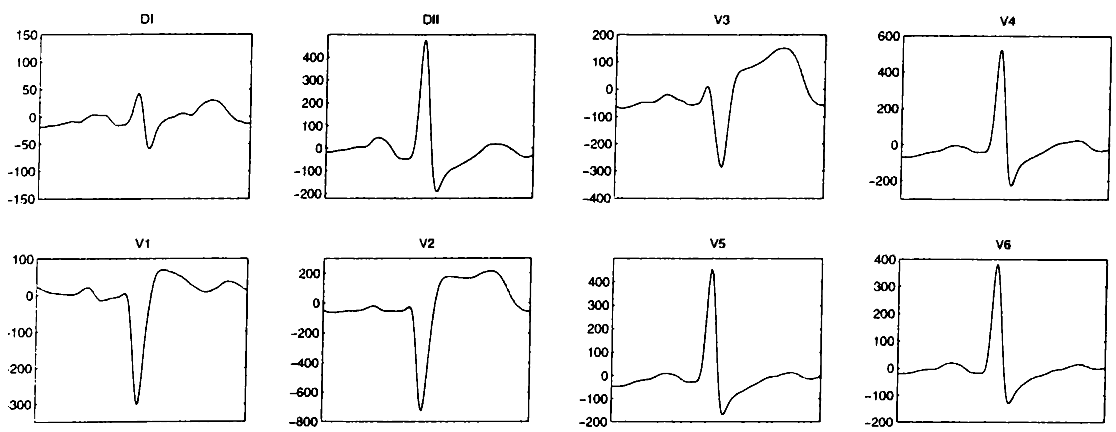

Figure 1.3: Typical waveforms recorded

In the stress ECG records, the most important part of the beat is the ST segment (see Figure 1.2). Its depression or elevation reveals important medical information about the heart and is only observable during an exercise test. Figure 1.4 shows a typical heart beat with depressed ST segment. The reference DC level is the part before the P wave and after the T wave.

The problem in stress ECG is the high noise that contaminate it. There are two predominant types of noise: **1.** Baseline wander noise (BW) and electrode motion artifact. **2.** Electromyogram-induced noise (EMG) [2]. BW is at a lower frequency, caused by respiration or motion of the patient or the leads. Frequency range of BW is usually below 0.5Hz and overlaps with that of the ST segment under stress. EMG noise, on the other hand, is at higher frequencies caused by increased muscle activity and by mechanical forces on

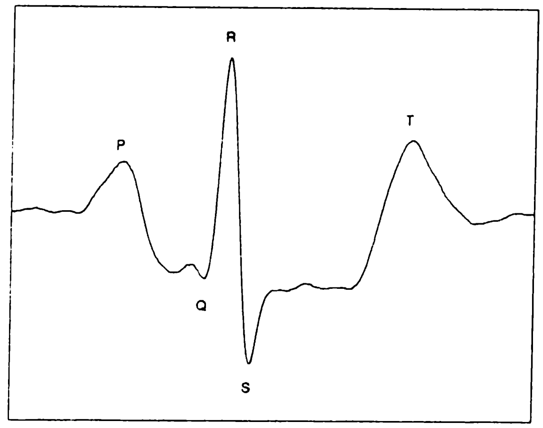

Figure 1.4: Heart beat with depressed ST segment

the electrodes. Its frequency range overlaps with that of ECG. Comparison of frequency spectra reveals the fact that direct filtering cannot be applied because it would distort ECG signal.

The stress ECG enhancing algorithms reported, compute a composite beat, an average beat in other words, and then make measurements on that beat. The following approaches can be found in the literature [3–8] :

Mean Composite: It is computed by averaging a set of noisy beats which are time aligned using a fiducial point, such as the peak of the R wave, in the heart beat. If the noise is uncorrelated with the signal, is stationary and has a Gaussian distribution, SNR is improved by $\sqrt{N}$ (N is the number of samples). However that is not the case, especially in stress ECG. If one of the beats has a sudden baseline shift or is an ectopic beat, a type of arrhythmia, the resulting composite will be distorted. So a preprocessing is needed.

Median Composite: It is determined by computing the median of sample values across a set of beats, for each time instant. Time alignment is also done. This technique removes any outliners thus is capable of removing baseline shift or bursts of high frequency noise. It is computationally involved.

Hybrid Composite: This approach combines the benefits of mean and median composite. A sequence of beats are grouped into three groups by one of the following strategies: **1.** Random grouping partitions beats into three random groups. **2.** Block grouping sequentially puts each one third into a group. **3.** Sequential grouping puts sequential beats into different groups. Arithmetic mean of each group is calculated. Then, estimated baseline level is subtracted from each mean and a low-pass filter with a cut-off frequency of about 15Hz is applied. The output makes up the low frequency (LF) signal.

The difference between the filtered and original composites make up the high frequency (HF) signal. Thus HF and LF average beats for each group are obtained. The median of the HF composites is summed with the median of the LF composites. This approach is near optimal for high frequency noise, good for low frequency noise and is computationally efficient.

Trimmed Mean Composite: It is computed by disregarding the bottom 20% and the top 20% of the sorted sample values for each time instant. Then the left are averaged. Thus it incorporates the feature of median filter by disregarding outliners and the feature of mean composite by taking averages, i.e. optimal when noise is Gaussian.

Incremental Composite: This approach is based on increasing or decreasing each sample value in the current (running) composite beat by a fixed amount. The direction of increment depends on the sample value of the next coming noisy beat with respect to the current composite. If it is higher, current composite's corresponding sample value is increased or vice versa. This approach provides a balance between immunity to noise and dynamic response of the composite.

Filter Bank [9]: This approach is based on a filter bank (FB) containing a set of analysis filters that decompose the input signal into several sub-bands and a set of synthesis filters that combine them to get the complete signal. Signal processing is done in between according to the application. Since signals contain specific energy distributions in frequency domain, time and frequency dependent processing is beneficial. FB allows this processing. There are some unavoidable distortions due to non-ideal transfer characteristics of the filters and due to aliasing.

Our approach, different than the previous approaches, depend on orthogonalization of input channels. The algorithm used for orthogonalization is a Singular Value Decomposition (SVD) based online orthogonalization algorithm. It was first applied to separate maternal and fetal ECG by Vanderschoot, et al. [1]. Input ECG channels are orthogonalized and less number of orthogonal channels which carry all the ECG information are produced. They have no redundancy. The use of correlations between the input channels, increases the noise immunity of decomposed signals. Moreover, EMG and BW are represented in the output channels which are orthogonal to the ECG containing ones. This is a computationally efficient method and runs online. This approach deals with each beat one by one with the aim of recovering all rather than directly disregarding outliner sample values or averaging.

The existing commercial ST analysis software uses composite beats to make measurements. Performance evaluation is done in the same way, using our algorithm as a preprocessing tool to enhance the ECG. Average beats of 20 second episodes are calculated and then analyzed. The enhancement we obtained allows beat by beat analysis of the ECG, but for comparison purposes, the existing method is preferred. As a result of noise elimination by orthogonalization, more beats can be detected. This means more beats are used in the computation of composite beats. Even during complete loss of a derivation we can generate that derivation from other signals with limited error. This provides an uninterrupted exercise ECG test. These improve the quality of analysis. 23 exercise ECG records whose length range from 9:00 min. to 21:20 min. are analyzed. Each data set contains 8 independently recorded ECG derivations, namely DI, DII, V1, V2, V3, V4, V5 and V6. ECG is sampled at 500 samples/sec. Data is quantized with a 12 bit A/D converter with a dynamic range of 12 mV. The conclusions and the decision rules reported are empirical. They are concluded after exhaustive analysis of these data sets.

Chapter 2

THEORY

2.1 SVD And Its Basic Properties

The concept of orthogonality is widely used in signal processing. Orthogonal subspaces contain independent information, thus avoid redundancy. Golub and Van Loan [10] make the definition of orthogonality as follows:

A set of vectors $\{\mathbf{x}_1, \ldots, \mathbf{x}_p\}$ *in* $\mathbf{R}^m$ *is orthogonal if* $\mathbf{x}_i^T\mathbf{x}_j = 0$ *whenever* $i \neq j$ *and orthonormal if* $\mathbf{x}_i^T\mathbf{x}_j = \delta_{ij}$*. If basis vectors of two subspaces are orthogonal to each other then they are called mutually orthogonal subspaces and contain maximally independent information. And a matrix* $\mathbf{Q}$ *is said to be orthogonal if* $\mathbf{Q}^T\mathbf{Q} = \mathbf{I}$.

The matrix 2-norm and Frobenius norms are invariant with respect to orthogonal transformations, i.e.

$$\|\mathbf{QAZ}\|_F = \|\mathbf{A}\|_F \quad (2.1)$$

$$\|\mathbf{QAZ}\|_2 = \|\mathbf{A}\|_2 \quad (2.2)$$

provided $\mathbf{Q}^T\mathbf{Q} = \mathbf{Z}^T\mathbf{Z} = \mathbf{I}$.

Among various orthogonal transformations, *Singular Value Decomposition (SVD)* is extremely useful concerning the information it provides about a given m-by-n real matrix:

If $\mathbf{A}$ *is a real m-by-n matrix then there exists orthonormal matrices*

$$\mathbf{U} = [\mathbf{u}_1\mathbf{u}_2\ldots\mathbf{u}_m] \in \mathbf{R}^{m \times n} \quad (2.3)$$
$$\mathbf{V} = [\mathbf{v}_1\mathbf{v}_2\ldots\mathbf{v}_n] \in \mathbf{R}^{n \times n} \quad (2.4)$$

such that

$$\mathbf{U}^T\mathbf{A}\mathbf{V} = \mathbf{\Sigma} = diag(\sigma_1, \sigma_2, \ldots, \sigma_p) \in \mathbf{R}^{p \times p}, \quad p = min(m, n) \quad (2.5)$$

where

$$\sigma_1 \geq \sigma_2 \geq \ldots \geq \sigma_p \geq 0$$

Proof can be found in [10].

U,**V** and $\mathbf{\Sigma}$ provide the following information about **A** at first [11]:

$$rank(\mathbf{A}) = k \qquad \sigma_{k+1} = \sigma_{k+2} = \ldots = \sigma_p = 0 \quad (2.6)$$
$$R(\mathbf{A}) = span(\mathbf{u}_1, \ldots, \mathbf{u}_k) \quad (2.7)$$
$$R^{\perp}(\mathbf{A}) = span(\mathbf{u}_{k+1}, \ldots, \mathbf{u}_m) \quad (2.8)$$
$$S(\mathbf{A}) = span(\mathbf{v}_1, \ldots, \mathbf{v}_k) \quad \text{solution space of } \mathbf{A} \quad (2.9)$$
$$N(\mathbf{A}) = span(\mathbf{v}_{k+1}, \ldots, \mathbf{v}_n) \quad (2.10)$$

There is an important relationship between SVD and the eigenvalue decomposition of the symmetric matrices $\mathbf{A}^T\mathbf{A}$ and $\mathbf{A}\mathbf{A}^T$. Since

$$\mathbf{x}^T\mathbf{A}^T\mathbf{A}\mathbf{x} = (\mathbf{A}\mathbf{x})^T(\mathbf{A}\mathbf{x}) = \|\mathbf{A}\mathbf{x}\| > 0 \quad (2.11)$$
$$\mathbf{x}^T\mathbf{A}\mathbf{A}^T\mathbf{x} = (\mathbf{A}^T\mathbf{x})^T(\mathbf{A}^T\mathbf{x}) = \|\mathbf{A}^T\mathbf{x}\| > 0 \quad (2.12)$$

both $\mathbf{A}^T\mathbf{A}$ and $\mathbf{A}\mathbf{A}^T$ are nonnegative definite, i.e. their eigenvalues are non-negative and their eigenvectors can be chosen to be orthonormal. So

$$\text{If } \mathbf{A} \in \mathbf{R}^{m \times n}, m > n \quad (2.13)$$

$$(\mathbf{A}^T\mathbf{A})\mathbf{V} = (\mathbf{U\Sigma V}^T)^T(\mathbf{U\Sigma V}^T)\mathbf{V} = \mathbf{V\Sigma}^T\mathbf{\Sigma} = \mathbf{V\Lambda} \tag{2.14}$$

$$(\mathbf{A}\mathbf{A}^T)\mathbf{U} = (\mathbf{U\Sigma V}^T)(\mathbf{U\Sigma V}^T)^T\mathbf{U} = \mathbf{U\Sigma\Sigma}^T = \mathbf{U}\begin{bmatrix} \mathbf{\Lambda} & \mathbf{0} \\ \mathbf{0} & \mathbf{0} \end{bmatrix} \tag{2.15}$$

$$\mathbf{\Lambda} = \mathbf{\Sigma}^T\mathbf{\Sigma} = diag(\sigma_1^2, \sigma_2^2, \ldots, \sigma_n^2) \tag{2.16}$$

We can conclude that the singular values of $\mathbf{A}$ are the square-roots of the first min(m,n) eigenvalues of $\mathbf{A}^T\mathbf{A}$ and $\mathbf{A}\mathbf{A}^T$. The left and the right singular vectors of $\mathbf{A}$ are the eigenvectors of $\mathbf{A}\mathbf{A}^T$ and $\mathbf{A}^T\mathbf{A}$ respectively [11].

The definition of rank can be misleading in the presence of noise. Rank decision gains crucial importance especially in an online algorithm where you do not have the full data matrix. SVD is a powerful tool for rank determination, because it provides information on how near a given matrix is to a matrix of lower rank [10]:

Let the SVD of $\mathbf{A} \in \mathbf{R}^{m\times n}$ *be given. If* $k < r = rank(\mathbf{A})$ *and*

$$\mathbf{A}_k = \sum_{i=1}^{k} \sigma_i \mathbf{u}_i \mathbf{v}_i^T \tag{2.17}$$

then

$$min_{rank(\mathbf{B})=k}\|\mathbf{A} - \mathbf{B}\|_2 = \|\mathbf{A} - \mathbf{A}_k\|_2 = \sigma_{k+1} \tag{2.18}$$

thus the definition

$$rank(\mathbf{A}, \epsilon) = min_{\|\mathbf{A}-\mathbf{B}\|_2 \leq \epsilon} rank(\mathbf{B}) \tag{2.19}$$

becomes

$$r_\epsilon = rank(\mathbf{A}, \epsilon) \Rightarrow \sigma_1 \geq \ldots \geq \sigma_{r_\epsilon} > \epsilon \geq \sigma_{r_\epsilon+1} \geq \ldots \geq \sigma_p \tag{2.20}$$

Finally we shall have a look at SVD related projections [10]:

Suppose

$$r = rank(\mathbf{A})$$

and

$$\mathbf{U} = [\mathbf{U}_r \widetilde{\mathbf{U}}_r] \qquad and \qquad \mathbf{V} = [\mathbf{V}_r \widetilde{\mathbf{V}}_r] \tag{2.21}$$

then

$$\begin{aligned}
\mathbf{V}_r \mathbf{V}_r^T &= projection \;\; onto \;\; null(\mathbf{A})^{\perp} \\
&= range(\mathbf{A}^T) && (2.22) \\
\widetilde{\mathbf{V}}_r \widetilde{\mathbf{V}}_r^T &= projection \;\; onto \;\; null(\mathbf{A}) && (2.23) \\
\mathbf{U}_r \mathbf{U}_r^T &= projection \;\; onto \;\; range(\mathbf{A}) && (2.24) \\
\widetilde{\mathbf{U}}_r \widetilde{\mathbf{U}}_r^T &= projection \;\; onto \;\; range(\mathbf{A})^{\perp} \\
&= null(\mathbf{A}^T) && (2.25)
\end{aligned}$$

Equation 2.24 will be the basis of the online algorithm.

2.2 Basis Of The Online Algorithm

2.2.1 Mathematical Basis [1]

Suppose that a measurement vector

$$\mathbf{m} = [m_1 m_2 \ldots m_p]^T \quad , \qquad \text{p=8 in our analysis} \tag{2.26}$$

is received at each time instant. The data matrix which is constructed by collecting all these vectors, $\mathbf{M}_{8 \times n}$, can be decomposed using SVD as

$$\mathbf{M} = \mathbf{U} \Sigma \mathbf{V}^T \tag{2.27}$$

It should be noted that for a given $\mathbf{M}$, the set of singular vectors, within a change of sign, and the singular values are unique provided that all singular values are distinct [11]. In case of equal singular values the singular vectors are not unique but the space spanned by them is.

A recursive property of each $\mathbf{u}_i$ is

$$\mathbf{u}_i^T \mathbf{M} = \sigma_i \mathbf{v}_i^T \tag{2.28}$$

$$\begin{gathered} \|\mathbf{M}^T \mathbf{x}\| / \|\mathbf{x}\| \leq \|\mathbf{M}^T \mathbf{u}_i\| = \sigma_i \\ \forall \mathbf{x} \in \mathbf{R}^p \ , \ \mathbf{x}^T \mathbf{u}_j = 0 \ , \ j = 1, \ldots, i-1 \end{gathered} \tag{2.29}$$

In words, $\mathbf{u}_i$ represents a filter in space for which the samples of the output signal reach a maximal rms value, where $\mathbf{u}_i$ is constrained to be orthogonal to $\mathbf{u}_1, \ldots, \mathbf{u}_{i-1}$. Physically, $\|\mathbf{M}^T \mathbf{u}_i\|$ represents the projected energy along $\mathbf{u}_i$. Remembering that $\mathbf{U}$ is orthogonal, we can use these filters to gather projected energy along orthogonal directions. $\mathbf{u}_1$ represents the highest energy containing direction, because it corresponds to the highest singular value, σ_1.

This is closely related to the rank problem. In ECG signals, the directions with small energy content are attributed to noise. The dimension of the rest gives the rank. This is precisely the effective rank determination. Given that the rank is r, the error made by excluding those dimensions is bounded by σ_{r+1} (see Equation 2.18).

If we can determine $\mathbf{U}_r$ (see Equation 2.21) then we can make use of the projection $\mathbf{U}_r \mathbf{U}_r^T$ onto range of $\mathbf{M}$.

The relation between the eigenvalue decomposition of a symmetric and positive definite matrix and SVD (see Equations 2.14 and 2.15) is used to determine $\mathbf{U}$. The online algorithm approximates $\mathbf{U}$ incrementally (see Section 2.2.2). Knowing r, rank($\mathbf{M}$), $\mathbf{U}_r$ is found from Equation 2.21.

2.2.2 Online Algorithm [1]

The strategy is to make an online eigenvalue decomposition of $\mathbf{M}\mathbf{M}^T$. Knowing that the subspace spanned by $\mathbf{U}$ (left singular vectors of $\mathbf{M}$) is invariant, it can be concluded that the subspaces spanned by $\mathbf{U}$ and $\mathbf{Q}_T$ (eigenvectors of $\mathbf{M}\mathbf{M}^T$) will be the same. Thus the problem becomes an eigenvalue decomposition problem of a nonnegative definite symmetric matrix.

$\mathbf{M}\mathbf{M}^T$ can be made diagonal by using a series of orthogonal transformations as in Equation 2.30. Each $\mathbf{Q}$ is a Givens Rotation matrix [10] and product of them make up Jacobi Rotation matrix [10]. This transformation makes $\mathbf{M}\mathbf{M}^T$ diagonal by making an off diagonal element zero at each step. In other words, it gathers the information on off diagonal entries onto diagonal entries. This property is due to the fact that it is itself an orthogonal transformation.

$$\mathbf{Q}^T_{\frac{p^2-p}{2}} \mathbf{Q}^T_{\frac{p^2-p}{2}-1} \cdots \mathbf{Q}^T_1 \underbrace{\mathbf{M}\mathbf{M}^T}_{\mathbf{C}} \mathbf{Q}_1 \cdots \mathbf{Q}_{\frac{p^2-p}{2}-1} \mathbf{Q}_{\frac{p^2-p}{2}} \tag{2.30}$$

where $\mathbf{Q}_k$ is the Givens rotation matrix given by

$$\mathbf{Q}_k = \begin{array}{c} \begin{array}{cc} \left[\begin{array}{cccccccc} 1 & 0 & & & & & \dots & 0 \\ 0 & & & & & & & \vdots \\ \vdots & & c & & & -s & & \vdots \\ \vdots & & & 1 & & & & \vdots \\ \vdots & & & & & & & \vdots \\ \vdots & & & & 1 & & & \vdots \\ \vdots & & s & & & c & & \vdots \\ \vdots & & & & & & & 0 \\ 0 & \dots & & & & & 0 & 1 \end{array}\right] & \begin{array}{c} \\ \\ i \\ \\ \\ \\ j \\ \\ \\ \end{array} \end{array} \\ \begin{array}{cccccccc} \quad & \quad & i & \quad & \quad & j & \quad & \quad \end{array} \end{array} \tag{2.31}$$

$$\mathbf{Q}_k^T \mathbf{Q}_k = \mathbf{I}$$

$$c = \cos\phi \qquad s = \sin\phi$$

$$2 \times \phi = \arctan \frac{2 \times c_{ij}}{c_{ii} - c_{jj}} \tag{2.32}$$

which makes c_{ij} and c_{ji} zero.

Due to uniqueness

$$span\left(\prod_{k=1}^{\frac{p^2-p}{2}} \mathbf{Q}_k\right) = span(\mathbf{U}) \tag{2.33}$$

However, since $\mathbf{M}$ is not known beforehand we approximate it by

$$\mathbf{M}_i = [\alpha^{i-1}\mathbf{m}(t_1) \dots \alpha\mathbf{m}(t_{i-1}) \ \ \mathbf{m}(t_i)] \tag{2.34}$$

where α serves as a memory element. At each time instant, t_i, we apply one Givens Rotation to make the maximum off diagonal element in absolute value, zero. Thus as $\mathbf{M}_i\mathbf{M}_i^T$ approaches to diagonal form, $\prod_{k=1}^{i} \mathbf{Q}_k$ approaches to $\mathbf{U}$.

The algorithm is:

$$\mathbf{U}_0 = \mathbf{I} \quad , \quad \mathbf{C}_0 = \mathbf{0} \tag{2.35}$$
$$for \quad i = 1 \quad to \quad n \tag{2.36}$$
$$\mathbf{s}_i = \mathbf{U}_{i-1}^T\mathbf{m}_i \tag{2.37}$$
$$\mathbf{B}_i = \alpha^2\mathbf{C}_{i-1} + \mathbf{s}_i\mathbf{s}_i^T \tag{2.38}$$
$$\mathbf{C}_i = \mathbf{Q}_i^T\mathbf{B}_i\mathbf{Q}_i \tag{2.39}$$
$$\mathbf{U}_i = \mathbf{U}_{i-1}\mathbf{Q}_i \tag{2.40}$$
$$\hat{\mathbf{m}}_i = \mathbf{U}_{i-1}[s_1 \ldots s_r 0 \ldots 0]^T \tag{2.41}$$

$\mathbf{Q}_i$ is the Givens Rotation matrix that makes the maximum off diagonal element of $\mathbf{B}_i$ zero. $\hat{\mathbf{m}}_i$ is the reconstructed vector (see Section 2.2.3).

α has a great effect on the performance of the algorithm (see Section 2.3.2). Good compromise were obtained with $\alpha = 1 - 2^{-13}$.

2.2.3 Effective Rank Of M

Effective rank of $\mathbf{M}$ is determined by tracing singular values and looking for a gap between two consecutive ones.

Physically r = rank($\mathbf{M}$) is the dimension of ECG information containing subspace. From now on this r dimensional subspace will be addressed as *Signal Space* and its orthogonal complement as *Noise Space.*

Reconstruction ignoring noise space yields noise-free, information dense signals. Reconstruction is done as

$$\hat{\mathbf{m}}_i = \mathbf{U}_{i-1}\hat{\mathbf{s}}_i \quad , \quad \hat{\mathbf{s}}_i = [s_1 \ldots s_r 0 \ldots\ldots 0]^T \tag{2.42}$$
$$\mathbf{s}_i = [s_1 \ldots s_r s_{r+1} \ldots s_p]^T$$
$$\hat{\mathbf{m}}_i = \mathbf{U}_{i-1}(\widehat{\mathbf{U}_{i-1}^T\mathbf{m}_i}) \tag{2.43}$$

This is the projection onto range of $\mathbf{M}$ (see equation 2.24). Figure 2.1 shows the input, decomposed and reconstructed data sets. There exist 8 channels in the input data set, but most of the ECG information in these channels are collected in 2 orthogonal channels after decomposition. All of the 8 input channels are reconstructed from these 2 orthogonal channels. The error made is limited by the QRS energy in the third and fourth decomposed signal channels.

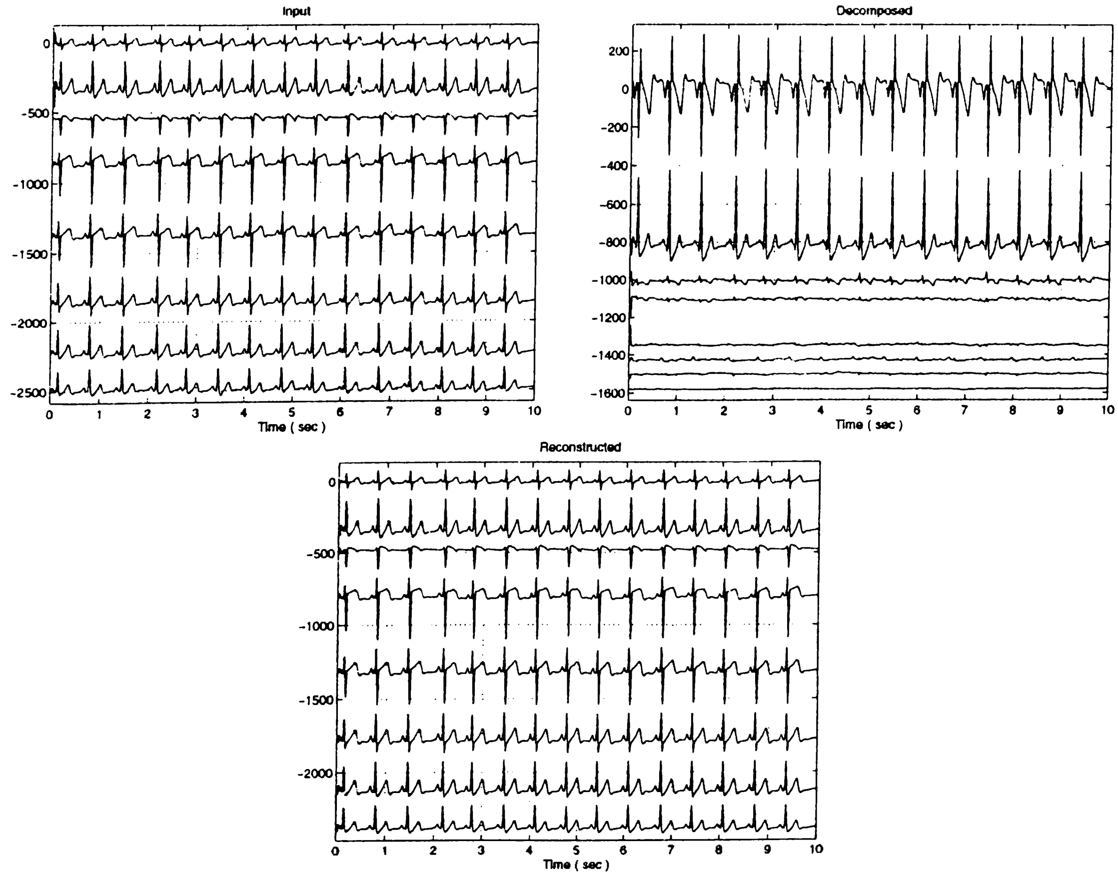

Figure 2.1: Input, decomposed and reconstructed signals
(The input and reconstructed channels are
in the order of DI, DII, V1,..., V6 throughout the text)

2.3 Some Properties Of The Algorithm

2.3.1 C Matrix

C corresponds to Σ^2. Since this is an online algorithm, whole data matrix is not available. At each instant a single data vector is received. **M** is approximated using these vectors as in Equation 2.34. This corresponds to updating the **C** matrix as in Equation 2.38.

Diagonal entries of **C** correspond to squares of singular values. They are representatives of the energy contained along the particular direction pointed by the corresponding $\mathbf{u}_i$. Rank determination (which is found after exhaustive analysis to be either 2 or 3 in ECG signals) is done based on these singular values.

The changes in the relative values of the diagonal entries of $\mathbf{C}$ are indications of changes of information content along specific directions. Such a change is instrumental as a noise alarm (see Section 2.4.4).

The singular values corresponding to signal space and noise space also show the quality of the data recorded. If the singular values corresponding to the signal space are significantly higher than the rest, then data is noise-free. In some cases, the signal components are not strong enough with respect to the noise components, causing noise to be interpreted as signal (see Section 2.3.4).

The off-diagonal entries of $\mathbf{C}$ correspond to cross correlations between the output SVD channels. Making $\mathbf{C}$ diagonal means orthogonalizing the output channels. The algorithm makes the maximum off-diagonal element in absolute value, zero at each step. In other words, it weakens the relation between maximally correlated output channels.

Since the structure of $\mathbf{C}$ determines the evolution of $\mathbf{U}$, we can direct $\mathbf{U}$ by manipulating $\mathbf{C}$:

Enforcing a rotation limit when c_{ij} is to be made zero, prevents $\mathbf{u}_i$ and $\mathbf{u}_j$ from rotating at the same time more than the applied threshold. Physically it means preserving the dependency between these two output SVD channels. This seems to be undesirable, however, if these two vectors are in the same subspace then their interdependence causes no problem concerning the information contained in that subspace. Such a threshold is applied for c_{12} when necessary (see Section 2.4.2).

A rotation limit, when applied on c_{ik} (for k=1,...,p), keeps $\mathbf{u}_i$ almost fixed. Thus we can preserve channels containing limited information to some extent. Figure 2.2 shows the effect of limiting c_{3k}. After enforcing a limit on c_{3k} the small ECG information present in the 3rd channel is kept in its place. The BW that contaminates the 3rd channel under limitless conditions, is shifted to the 4th channel.

If the structure of $\mathbf{C}$ is changed externally, the decomposed output signal set manipulates itself accordingly. This effect is extreme if the diagonal entries of $\mathbf{C}$ are reordered. After such a reordering the order of the output signals also change in the same way. Figure 2.3 shows the decomposed signal set when the

1st and 3rd diagonal entries of **C** are interchanged at 2nd sec. Within 10 sec. the 1st and 3rd SVD channels change place in accordance with the change in the diagonal entries.

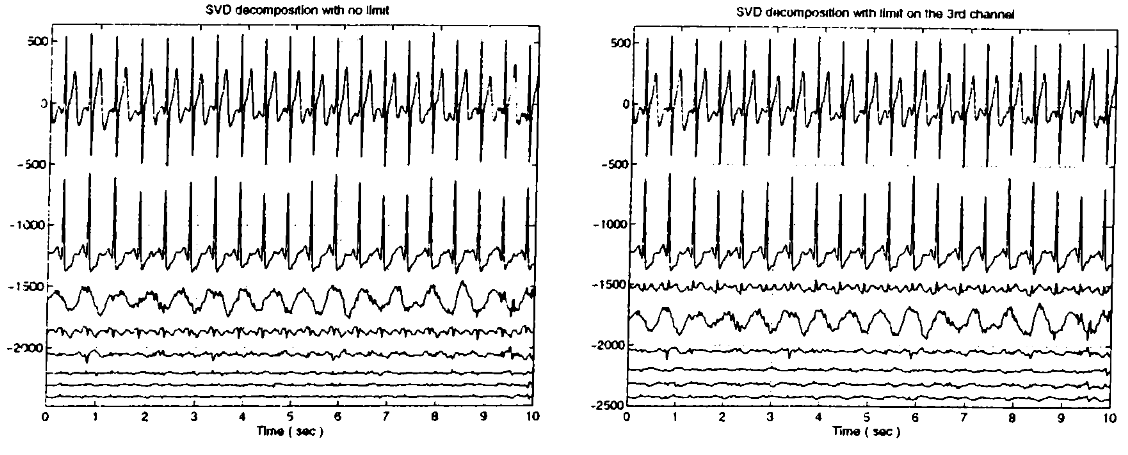

Figure 2.2: Effect of limiting the 3rd SVD channel

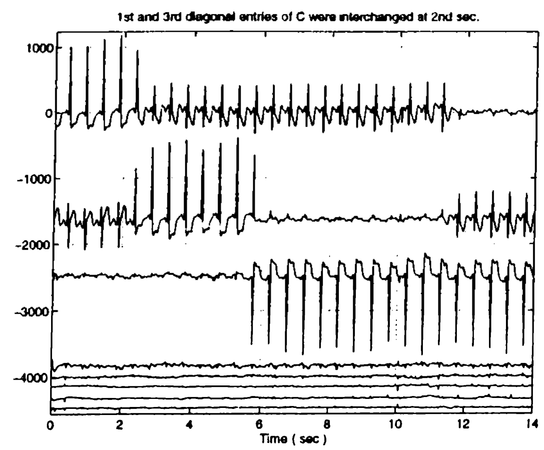

Figure 2.3: Decomposed signals when c_{11} and c_{33} were interchanged

2.3.2 Memory Factor , α

α determines how far the algorithm remembers the past data. Good compromise are obtained with $\alpha = 1 - 2^{-13}$.

If it is too high then the algorithm loses its flexibility and cannot trace the changes in ECG signals. The **u** vectors remain almost fixed because **C** is not changed much with each coming data vector. If it is too low then, in the presence of noise, it cannot preserve the signal space even for a short time. It interprets noise as signal. Even QRS complexes may cause rotations of **u**'s under noise-free conditions.

Figure 2.4 shows the decomposed signals of the same input data set with different α values, $1-2^{-13}$ and $1-2^{-8}$ respectively. For small α values, the algorithm cannot preserve the ECG signals and they shift in between output channels.

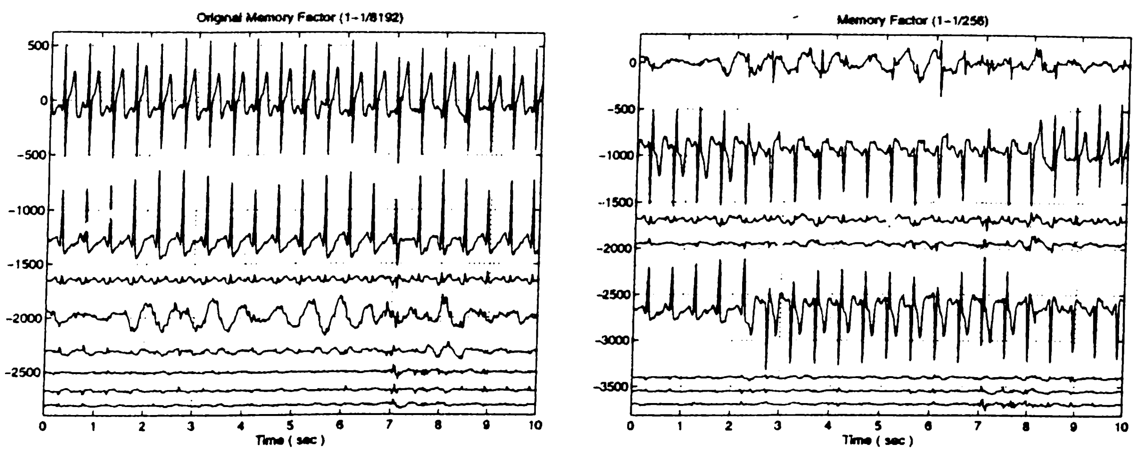

Figure 2.4: SVD with different α values

2.3.3 The Q Matrix

Product of all $\mathbf{Q}_k$'s is called the *Jacobi Rotations Matrix* [10] (see Equation 2.30). It is the same as Givens Rotations. $\mathbf{Q}$, as given in Section 2.2.2, performs a rotation of the vectors $\mathbf{u}_i$ and $\mathbf{u}_j$ in clockwise direction with an angle ϕ on the plane defined by $\mathbf{u}_i$ and $\mathbf{u}_j$, as in Figure 2.5. In the algorithm, i and j are chosen to be the indices of the maximum off-diagonal entry of $\mathbf{C}$ in absolute value.

ϕ is chosen such that after the following transformation

$$\mathbf{Q}^T\mathbf{C}\mathbf{Q} = \mathbf{C}' \tag{2.44}$$

C's maximum off diagonal element is made zero. Since

$$\mathbf{Q}^T\mathbf{Q} = \mathbf{I} \tag{2.45}$$

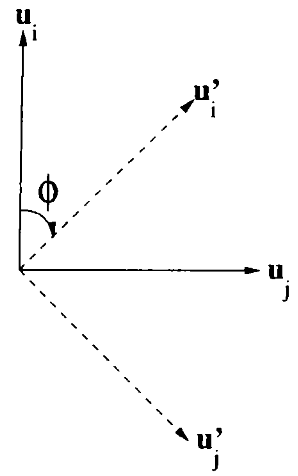

Figure 2.5: Rotation of **u**'s

this transformation is an orthogonal transformation. We do not lose any information present in **C**

If ϕ is limited, smaller rotations will occur. This will result in non-zero results for the chosen off-diagonal entry of **C**.

2.3.4 Importance Of DII

Algorithm is very sensitive to noise in DII because it is the least redundant input channel due to its spatial position on the body (DIII is evaluated from DI and DII). Figure 2.6 shows the positions of D derivations on the body.

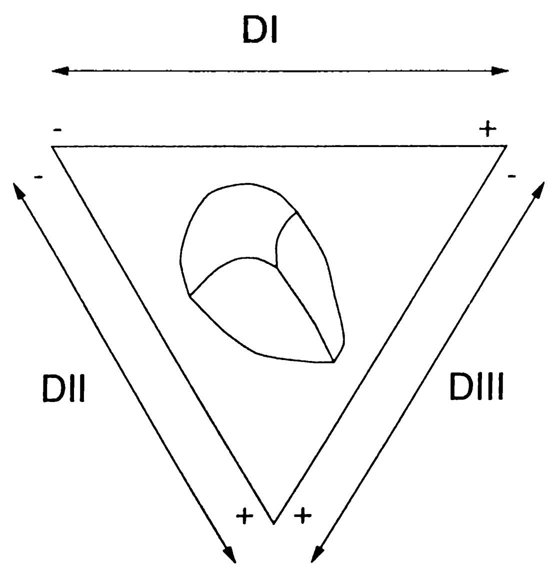

Figure 2.6: Leads of D derivations in ECG

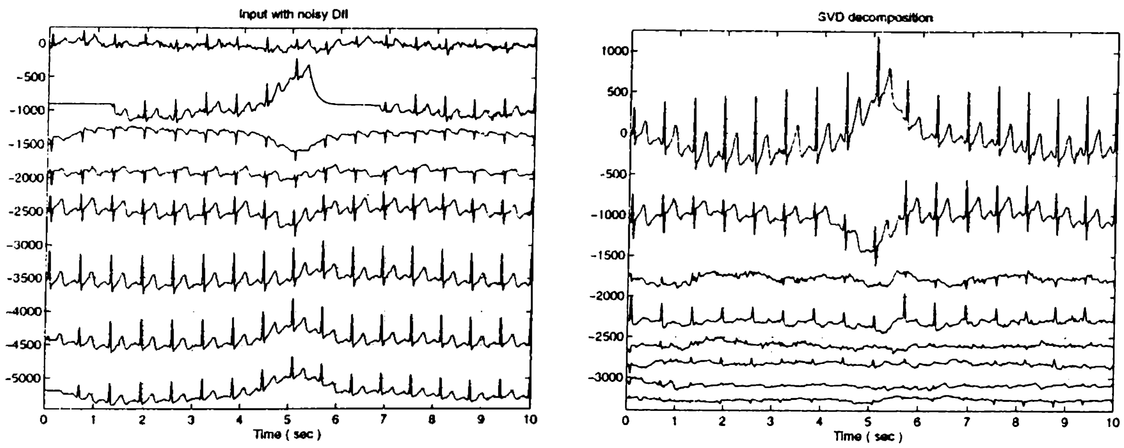

Figure 2.7: Input and decomposed signals when DII is noisy

The leads on the body used to record ECG signals, record the potential differences occuring on the surface of the body due to the action potentials on heart. Heart can be thought as a dipole with some specific orientation. The currents on it flow in accordance with this orientation. DII is the only lead that is concerned with the currents' projection on the direction from right arm to left leg (same as the position of heart in the body). If DIII were recorded independently, this dependence on DII could be lowered because only then there would be an alternative input channel to DII. Figure 2.7 is an example of the performance of the algorithm in case of undesirable DII. The high noise in DII is completely observable in the most significant SVD output channel, the 1st channel.

Generally, if QRS is seen in the third SVD output channel, this comes from DII. Because of this if noise accumulation is detected at the third SVD channel during noise detection (see Section 2.4.4) (and if that channel is a QRS containing channel), DII is selected as noisy input channel at first. This choice is obviously a first estimate and may be erroneous. Such an error is preferred to missing noise because we can reconstruct the excluded input channel, though with limited error. Including DIII into the input data set as an independently recorded signal would reduce such errors by increasing redundancy.

2.4 The Method

The program is implemented in Borland C++ under Windows 3.1.1. And it was run in 486 DX 4 IBM compatible PC. The flow chart of the program is given in Figure 2.8. The explanations about the specific parts follow.

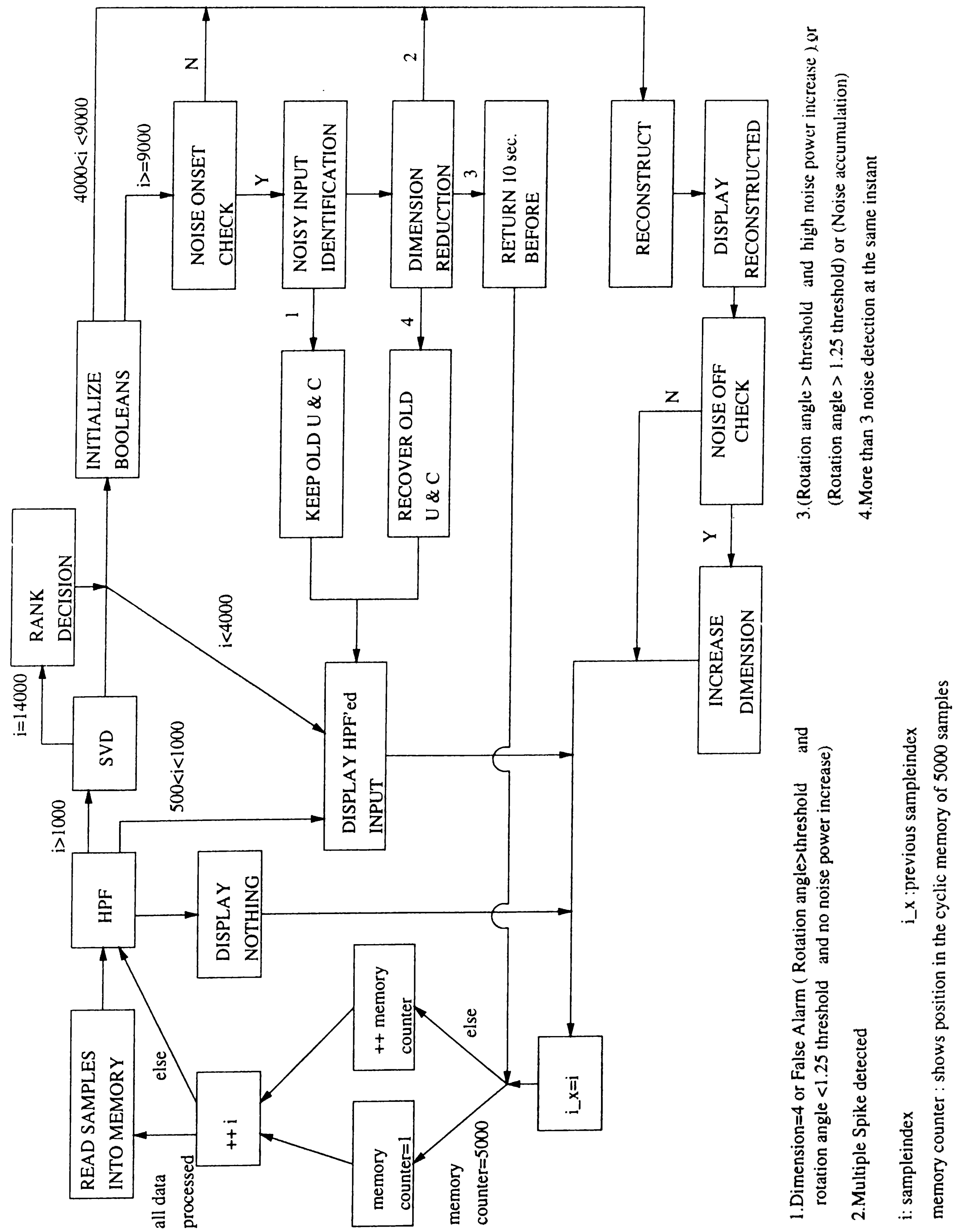

Figure 2.8: Flow Chart

2.4.1 High Pass Filter

SVD is sensitive to DC components in input signals. DC is interpreted as a signal component and number of QRS containing output channels increases to represent the DC in the input. This leads to an increase in rank and inefficient compression of information. Figure 2.9 demonstrates the effect of non-zero DC in the input, on the output. The number of orthogonal signal channels is more than it should be when HPF is not applied. Note that the extra channel contains QRS complexes with almost the same morphology with the first SVD channel. This means that the 3rd channel exists only to represent DC.

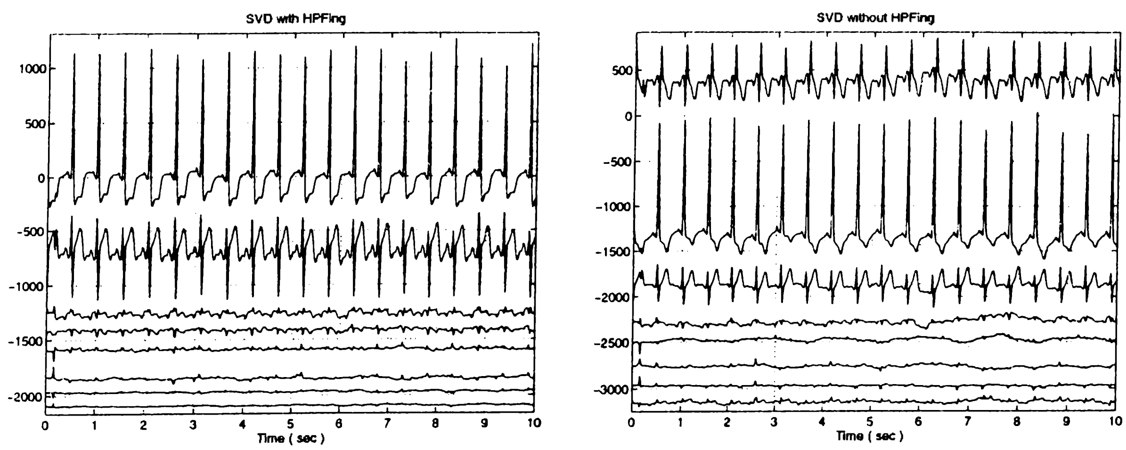

Figure 2.9: Effect of DC

To avoid those redundant output channels, a first order Butterworth high pass filter with a cut-off frequency of 0.7 Hz, is applied to the input. Besides DC, very low frequency baseline variations are also eliminated. Since the filter is first order, it does not change the morphology of the signal significantly and is fast.

For faster operation, the coefficients were selected to be powers of 2. The transfer function of the filter used is

$$H(z) = \frac{(1-2^{-7}) - (1-2^{-7})z^{-1}}{1-(1-2^{-6})z^{-1}} \tag{2.46}$$

Figure 2.10 shows the magnitude and phase response of that high pass filter.

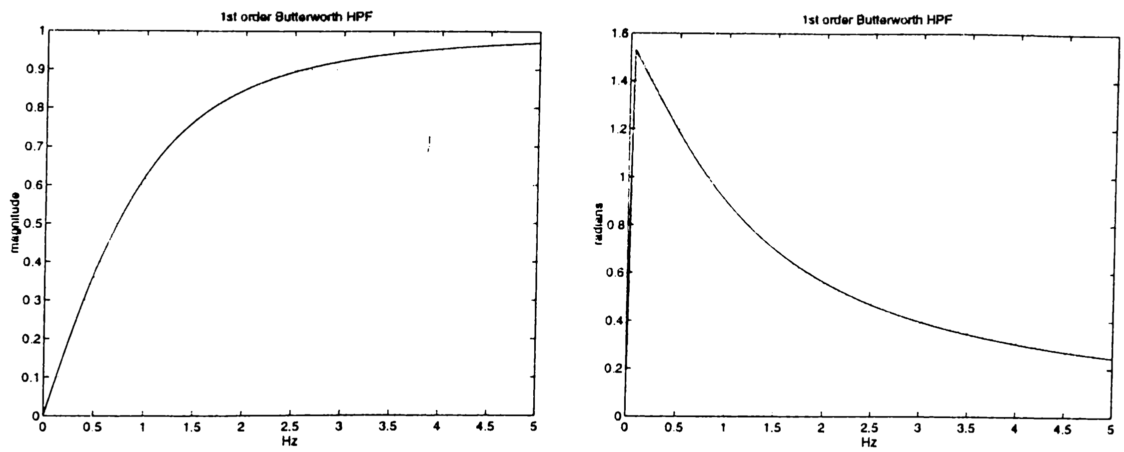

Figure 2.10: High Pass Filter characteristics

2.4.2 Orthogonalization

The algorithm given in Equations 2.35 to 2.40 is implemented in this step. Only the reconstruction, Equation 2.41, is left to other steps.

Before creating $\mathbf{Q}_i$, it finds the maximum off diagonal element. Since $\mathbf{B}_i$ is symmetric, a search algorithm may choose (i,j) or (j,i) equivalently. The difference will be in the sign of rotation angle , ϕ , computed (see Equation 2.32) because c_{ii}'s are in order of magnitude. We search in such a way that c_{ii} is always greater than c_{jj}. Thus, sign of ϕ is only dependent on the sign of c_{ij} chosen.

If rank is 3 , that is, if we need the third SVD output channel during reconstruction, we limit ϕ when $c_{3k}(k = 1, \ldots, 8)$ is chosen to be made zero. This limits the rotation of $\mathbf{u}_3$. It is necessary because in any case the third SVD channel is a low energy containing one and is not immune to noise.

Besides, if energy in the first and second SVD channels are close to each other we limit c_{12}, that is simultaneous rotation of $\mathbf{u}_1$ and $\mathbf{u}_2$ is prevented. This is done because when they are close to each other in the energy content, it is very likely that c_{12} will be the maximum off-diagonal element most of the time. That will cause $\mathbf{u}_1$ and $\mathbf{u}_2$ to rotate simultaneously. Their rotation does not make any difference considering the reconstruction process because signal components are still kept in the signal space. Such rotations, on the other hand, cause false noise alarms.

The bound applied to ϕ is $0.001°$ in absolute value. This value was found empirically. It corresponds to 5° of rotation at maximum between two consecutive noise checks. This is the maximum rotation angle observed in most of the data under noise free conditions. Thus, our limiting causes the rotation to be more homogeneous rather than avoiding rotation completely.

Angle limiting is not a preferred method because tracing the rotation direction of **u** vectors performs best in the absence of such limits. It is also the most secure way of noisy input channel identification.

The program decides on limiting ϕ or not, at the stage of Rank Decision (see Section 2.4.3). The relative energy content of the output SVD channels is checked by inspecting the diagonal entries of **C**, to decide on the limits to be applied. Weak signal channels are preserved by enforcing rotation limits on them. Strong ones are left free. The rotations in between strong signal channels are limited to avoid redundant rotations because they cause false noise alarms.

2.4.3 Rank Decision

First 30 seconds of the data is assumed to be noise free. Parameters are set according to the values at the 28th second.

Exhaustive analysis of ECG records showed that the rank of **M** is 2 and in few cases it is 3. This means information in ECG signals can be represented in 2 independent channels. So we are only concerned with c_{33} to decide on the rank.

The high amount of ECG information containing channels are named as signal channels. The decided effective rank is used to determine the number of signal channels. They are checked for their rotations during noise detection. The rest of the channels are named as noise channels. Their rotation is not important. Noise channels are checked against noise accumulation (see Section 2.4.4). If high noise energy accumulates in one of them, then that channel interferes with a signal channel.

In some cases, even though the effective rank of **M** is decided to be 2, the ECG information content of the 3rd channel cannot be disregarded. In such cases, although the highest energy containing 2 SVD channels are taken to be the signal channels, the 3rd channel is also included in the reconstruction. This 3rd channel is checked against noise accumulation, as if it is a noise channel. Whenever the 3rd SVD output channel is included in the reconstruction, c_{3k}

($k = 1, \ldots, 8$) is limited to preserve the low energy ECG signal on it.

If the energy content of the 1st and 2nd SVD output channels are close to each other, it is very likely that c_{12} will be chosen as the maximum off diagonal element of $\mathbf{C}$ most of the time. This causes simultaneous rotations of $\mathbf{u}_1$ and $\mathbf{u}_2$. Such rotations do not cause loss of ECG because these 2 signals are in the same subspace, signal space, but they cause false noise alarms. In such data sets, rotation angle, ϕ, when c_{12} is chosen to be made zero, is bounded. This limit prevents $\mathbf{u}_1$ and $\mathbf{u}_2$ from rotating at the same time, avoiding false noise alarms. This limitation also causes an inefficient orthogonalization of these 2 channels. They remain somewhat correlated but this does not cause information loss (see Section 2.4.2).

Generally noise accumulation check is done with respect to c_{22} as it is the weakest signal channel. In some cases, the 2nd SVD channel is so weak that, noise accumulation check with respect to that channel causes frequent noise alarms. Most of them turn out to be false alarms. Then, noise accumulation check has to be done with respect to c_{11}. The decision is given by checking c_{22}. Figure 2.11 shows the highest 3 diagonal entries of the data sets analyzed at the time of rank decision, i.e. at the end of the training step.

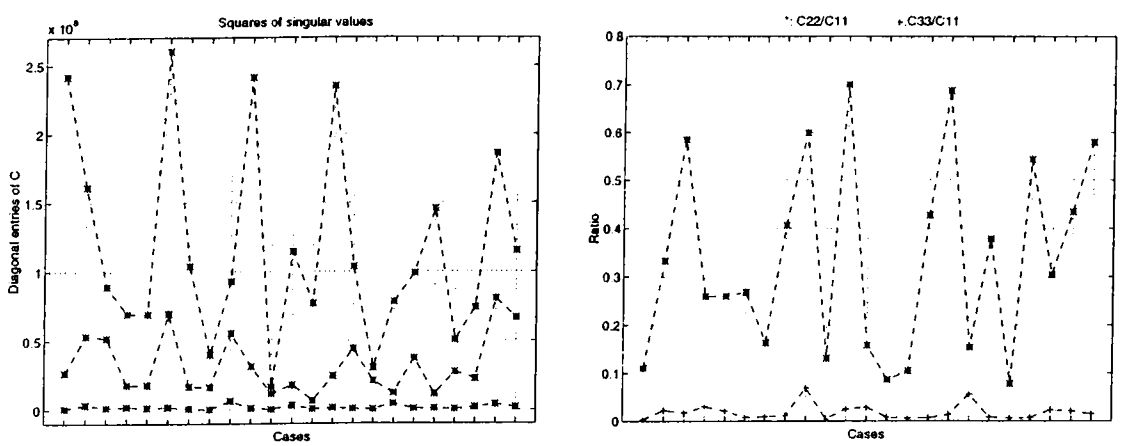

Figure 2.11: Diagonal entries of $\mathbf{C}$

Whenever a rotation angle limit is applied, or there is extraordinarily high energy content in an SVD channel, the angle thresholds, used in noise detection, has to be readjusted.

These checks need to be done independently. None of them implies another one. For example, deciding on a rank 2 condition does not imply that 2 SVD channels are enough to keep all the ECG information. There are cases like reconstructing from 3 SVD channels when the decided effective rank is 2. The following decision rules are found empirically after intensive analysis of 23 exercise ECG data sets of length ranging from 9:00 min. to 21:20 min.

The default settings are: No limit on rotations is applied, SVD and reconstruction are done for 2 channel conditions, rotation angle threshold for the first SVD channel is 0.31 radians (th_1) and for the second SVD channel it is 0.40 radians (th_2), noise accumulation check is done with respect to the second SVD channel.

The checks are done in the given order and necessary readjustments are done accordingly.

$$c_{22} > 0.3448 \times c_{11} \Longrightarrow \text{Limit } c_{12} \Longrightarrow \text{th}_1 = 0.20 \text{ rad. ,th}_2 = 0.35 \text{ rad.}$$

i.e. the 1st and 2nd SVD channels are so close to each other that rotations in between them are likely. They can cause false noise alarms. Even though this limitation avoids their being orthogonal to each other to some extent, this is not important because we keep the ECG signals in the signal space.

$$c_{33} > 0.04 \times c_{11} \Longrightarrow \text{reconstruction from 3 channels} \Longrightarrow \text{Limit } c_{3k}$$

i.e. the 3rd SVD channel should be used in reconstruction. The corresponding basis vector must be kept fixed with some threshold to keep the information on it.

$$c_{33} > 0.25 \times c_{22} \Longrightarrow \text{rank}(\mathbf{M}) = 3 \Longrightarrow \text{No rotation limiting}$$

i.e. the 3rd SVD channel carries information comparable to the 2nd SVD channel's. So it will be used in reconstruction. The noise effect on $\mathbf{u}_3$ can be detected from its rotation just like the 1st and 2nd SVD channels. The angle threshold used for the 3rd channel is th_2.

$$c_{22} < 0.09 \times 10^8 \Longrightarrow \text{Do noise accumulation check wrt 1st SVD channel}$$

i.e the 2nd SVD channel does not contain much ECG energy, hence noise energy should be compared with the energy of the 1st SVD channel to detect noise accumulation.

$$\text{rank}(\mathbf{M}) = 2 \Longrightarrow c_{22} > 7.00 \times 10^8 \Longrightarrow th_1 = 0.10 \text{ rad. , } th_2 = 0.15 \text{ rad.}$$

i.e. ECG energy in the 2nd channel is so high that smaller rotations can cause signal vectors to take on noise. The thresholds are lowered.

These thresholds, used in decisions, depend on α. Since clinical data were used to determine the above rules, they reflect the real values that one can come across. The readjustments made, improve the performance of the program, especially its noise detection capability. The ST analysis results reported in Section 3.2 were obtained by applying these rules.

In general, it is concluded that the ECG signals can be represented in 2 orthogonal channels with enough accuracy for Exercise ECG Test.

2.4.4 Noise Detection

In order of importance, rotation of the basis vectors of the signal space, noise accumulation in the most significant noise channel (in case of reconstruction from 3 channels when rank($\mathbf{M}$)=2, the third signal channel is also checked for noise accumulation) and total noise energy increase are checked at every 10 seconds.

First, rotation of the basis vectors is checked. If anyone of them has rotated more than the corresponding threshold, this indicates that the rotated basis vector began to take on noise. Signal space's basis vectors are highly stable and do not rotate much in the absence of noise. Thresholds applied are:

If c_{12} is limited , the threshold for $\mathbf{u}_1$ is 0.20 radians, and 0.35 radians for $\mathbf{u}_2$ and $\mathbf{u}_3$. If c_{12} is not limited then these limits are 0.31 radians and 0.40 radians respectively. If $c_{22} < 7.00 \times 10^8$ (see section 2.4.3) then they are 0.10 radians and 0.15 radians respectively. Threshold for $\mathbf{u}_1$ is less then the others because although it is more stable, its smaller rotation causes more loss of information. So we have to be more careful in watching $\mathbf{u}_1$. Note that when rotations are limited, thresholds are lower not to miss noise.

When a rotation more than the threshold occurs, total noise energy increase is checked. If it has not increased at least 1.5 folds within the last 10 seconds then alarm is considered to be false. The assumption here is that if noise arrives, it cannot be represented completely in the signal space. Energy of the noise channels must also increase.

Against the possibility of noise being observable completely in signal space, we check the rotation angles against 1.25$\times$threshold. If such a high rotation has occured then it is decided on the existence of noise directly, without checking the total noise energy increase.

If vector rotation is not detected then noise accumulation is checked. Low frequency, high amplitude noise do not rotate signal space vectors significantly but accumulate in a noise channel for some time. When the corresponding diagonal entry of **C** gets high enough, noise interferes with the signal space. At that instant, we cannot identify the noisy input channel. So all we can do is to detect such an accumulation on the most significant noise channel when it starts and identify noisy input channel from the corresponding **u**.

Figure 2.12 shows an example of noise accumulation. The BW in the 3rd SVD channel interferes with the signal in the 2nd SVD channel after 30 seconds. The energy of the 2nd channel and BW are close to each other and as a result the algorithm cannot keep them separated for more than 15 sec. This is same as interchanging the 2nd and the 3rd diagonal entries (see Figure 2.3).

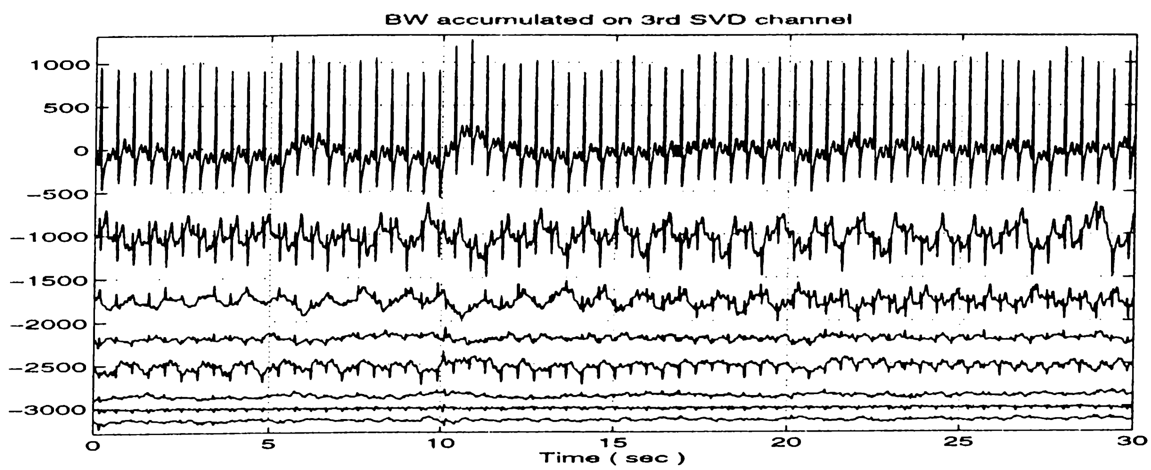

Figure 2.12: Noise Accumulation

Accumulation detection is done as follows:

If $$c_{kk} > 0.24c_{tt}$$

$$c_{kk} = max(c_{(r+1)(r+1)}, \ldots, c_{88}) \ , \ r = rank(\mathbf{M})$$
$$t = \begin{cases} 1 & c_{22} < 0.09 \times 10^8 \\ 2 & c_{22} \geq 0.09 \times 10^8 \end{cases}$$

then it is decided that noise has accumulated on k^{th} SVD channel.

Accumulation check is done with respect to c_{11} or c_{22} rather than c_{rr} because even when r=3 , energy in the third channel may be close to noise energy. This check is not indicative in that case. Noise may not be observable in the third SVD channel.

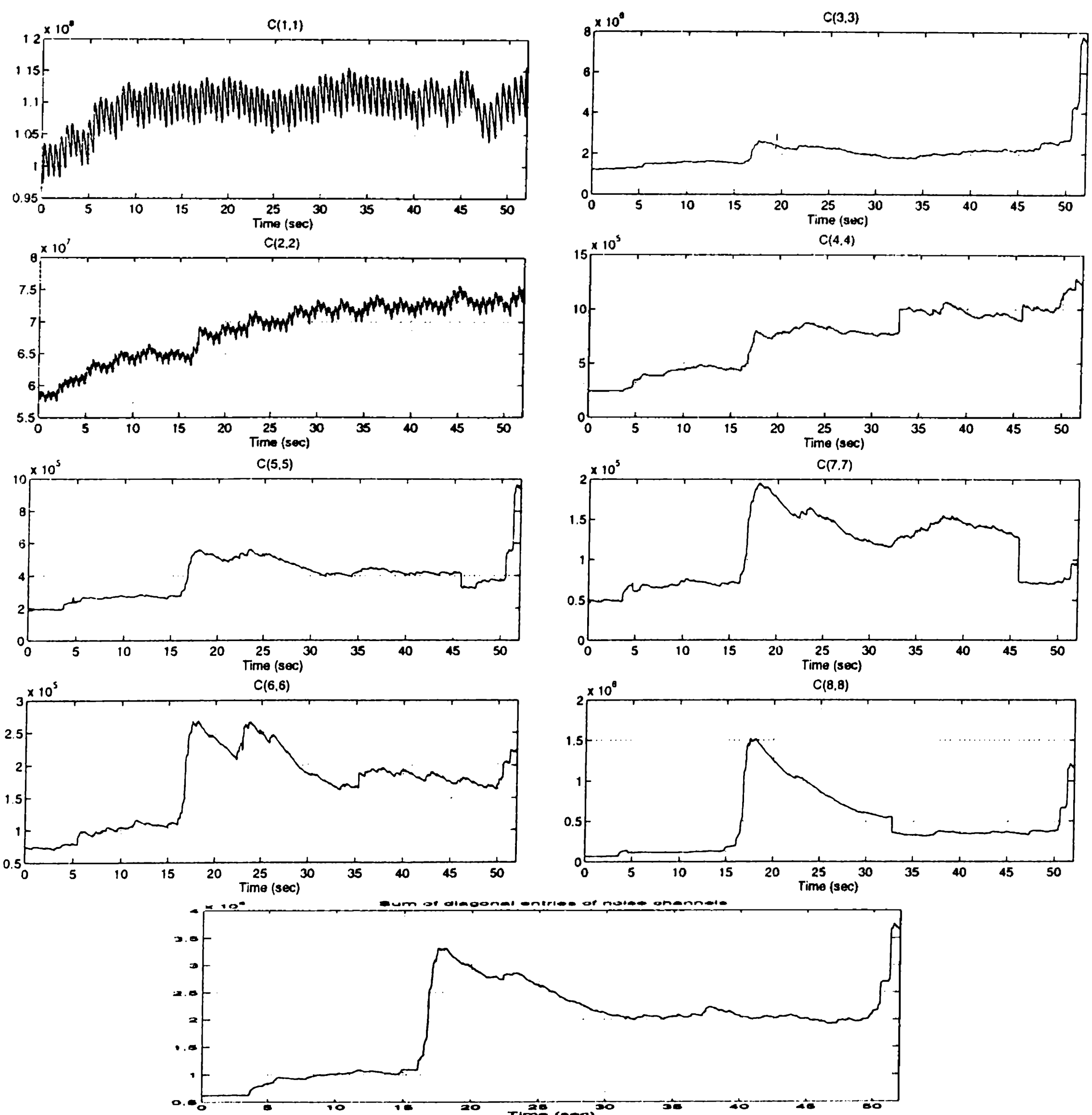

Figure 2.13: Energy content of SVD channels

A multiple spike (spike in most of the input channels, usually in all) check is also applied. During the experiments , it was observed that if a spike (short duration, even instantaneous, high amplitude noise) arrives, total noise energy graphic exhibits a jump and then falls to its old value rapidly. This fast fall is detected. If slope is over a threshold of $64\text{mV}^2/\text{sec}$ then it is considered as a multiple spike, no dimension reduction is applied, old **U** and **C** are recovered to avoid the rotation effect of it.

Figure 2.13 shows the graphics of diagonal entries of **C** of EMG contaminated exercise ECG data set. The time when the noise starts is the time when the jump in the graphics corresponding to noise channels, occurs.

2.4.5 Noisy Input Channel Identification

Noise is detected in two ways, either signal vectors rotate more than a threshold or noise accumulates on a noise vector or on $\mathbf{u}_3$ as a special case ($\mathbf{u}_3$ is considered as a noise or signal vector depending on the energy it collects).

The former is an abrupt change. If the cause of noise detection is a rotation then we look for the direction of rotation. The vector rotates to take on noise. The component of the vector which experienced maximum increase in absolute value corresponds to the noisy input channel.

The latter is a slowly evolving change. At the time of accumulation detection, it has already directed towards the noise. That is, the vector's maximum component in absolute value shows the noisy input channel. The direction of rotation within the last 10 seconds can be misleading in such a situation because the vector usually tries to turn towards the clean input channels during accumulation. If it succeeds then no accumulation occurs.

2.4.6 Dimension Reduction

Since

$$\mathbf{s} = \mathbf{U}^T\mathbf{m} \tag{2.47}$$

the rows of $\mathbf{U}$ can be associated with input channels whereas the columns with the output SVD channels.

Decreasing dimension by one means deleting the selected input channel and an output channel. The input channel is selected by *noisy channel identification* (see Section 2.4.5). The output channel is always selected to be the weakest SVD channel, i.e. the last noise channel. The corresponding row and column are deleted from $\mathbf{U}$. The new $\mathbf{U}$ is re-orthogonalized by *Gramschmidt Method* [12] to maintain orthogonality. This process starts with the leftmost column of $\mathbf{U}$, keeping it unchanged (the highest energy containing signal vector), proceeds towards the weakest noise vector.

The rows and columns of $\mathbf{C}$ correspond to the output SVD channels. The last row and column of $\mathbf{C}$ are also deleted.

If the k^{th} input channel is to be excluded when the current dimension is l, the rows and columns shown by $*$ in the following are deleted.

$$\mathbf{U}_l = \begin{array}{cc} \begin{bmatrix} & & & & * \\ * & * & * & * & * \\ & & & & * \\ & & & & * \\ & & & & * \end{bmatrix} & \begin{array}{c} \\ k \\ \\ \\ \\ \end{array} \\ \begin{array}{ccccc} \quad & \quad & \quad & \quad & l \end{array} & \end{array}$$

$$\mathbf{C}_l = \begin{array}{cc} \begin{bmatrix} & & & & * \\ & & & & * \\ & & & & * \\ & & & & * \\ * & * & * & * & * \end{bmatrix} & \begin{array}{c} \\ \\ \\ \\ l \end{array} \\ \begin{array}{ccccc} \quad & \quad & \quad & \quad & l \end{array} & \end{array}$$

2.4.7 Noise-Off Check And Dimension Increase

At every 10 seconds, two peaks are found at each input channel towards past. If ECG is noise-free then these two peaks are R peaks of QRS complexes (For input channels V1, V2 ,V3 minimums rather than maximums are found due to their morphologies (See Figure 1.3)). Duration of a QRS is around 0.2 seconds which corresponds to 100 samples. Total error between time intervals of 0.2 sec. around these two peaks is calculated. Then a threshold is applied to its ratio with the QRS energy of that channel. The applied threshold is determined for each channel during training. They are bounded by a minimum of 0.2 and a maximum of 0.8. Too high thresholds would result in false *noise-off* decisions. Too low ones would miss noise-off. Bounds are put to avoid these.

Whenever noise-off is found, the most recent 8 dimensional **U** and **C** are reduced in dimension excluding the still noisy input channels. Reconstruction coefficients are also updated according to the new **U**.

2.4.8 Reconstruction

Since **U** is an orthogonal matrix

$$\mathbf{U}^{-1} = \mathbf{U}^T \ , \ \mathbf{m} = \mathbf{U}(\mathbf{U}^T\mathbf{m}) = \mathbf{U}\mathbf{s} \tag{2.48}$$

Equation 2.48 reconstructs the input channels from SVD outputs identically.

To exclude the orthogonal noise components during this reconstruction , $\hat{\mathbf{s}}$ is used instead of $\mathbf{s}$, i.e. we exclude noise channels from the decomposed vector. In noise free conditions , these channels are almost zero. Thus we guarantee that we do not exclude ECG information.

$$\hat{\mathbf{s}} = \begin{bmatrix} s_1 & s_2 & & s_r & 0 & \ldots & 0 \end{bmatrix}^T \qquad r = 2,3 \tag{2.49}$$

$$\hat{\mathbf{m}} = \mathbf{U}\hat{\mathbf{s}} \tag{2.50}$$

Reconstruction from 2 or 3 channels depends on the rank of the data processed. Although, usually two channels are used, in some cases 3 channel reconstruction becomes a must. In 2 channel reconstruction, we sacrifice some QRS energy that is left in the third channel, to exclude noise. The examples in Figure 2.14 are noise-free cases so the sacrificed QRS energy is fully observable. The differences mainly occur in the amplitudes of the peaks. Avoiding noisy output was preferred to capturing all QRS energy in noisy parts. The lost QRS energy is not much and not significant for ST analysis in Exercise ECG Test. The difference mainly occurs at the amplitude of the R-wave. Table 2.1 gives the energies of the original QRS complexes and reconstructed ones under noise-free conditions. They are computed by

$$\Sigma_{k=1}^{100} m_k^2 \quad , \quad m_k \text{ is the } k^{th} \text{ sample value}$$

Channel	*QRS SS*	*2 ch. rec. SS*	*3 ch. rec. SS*
DI	288	278	300
DII	1803	1703	1812
V1	1263	1226	1290
V2	4029	3911	4044
V3	14422	14575	14440
V4	3654	3355	3546
V5	2049	1885	2010
V6	3331	3276	3275

Table 2.1: Comparison of 2 and 3 channel reconstructed QRS energies
SS : Sum of Squares

Figure 2.15 shows a comparison of the reconstructed ECG signals by using SVD coefficients and LMS-Newton [13] coefficients, from the most significant 2 SVD output channels . The LMS-Newton algorithm is

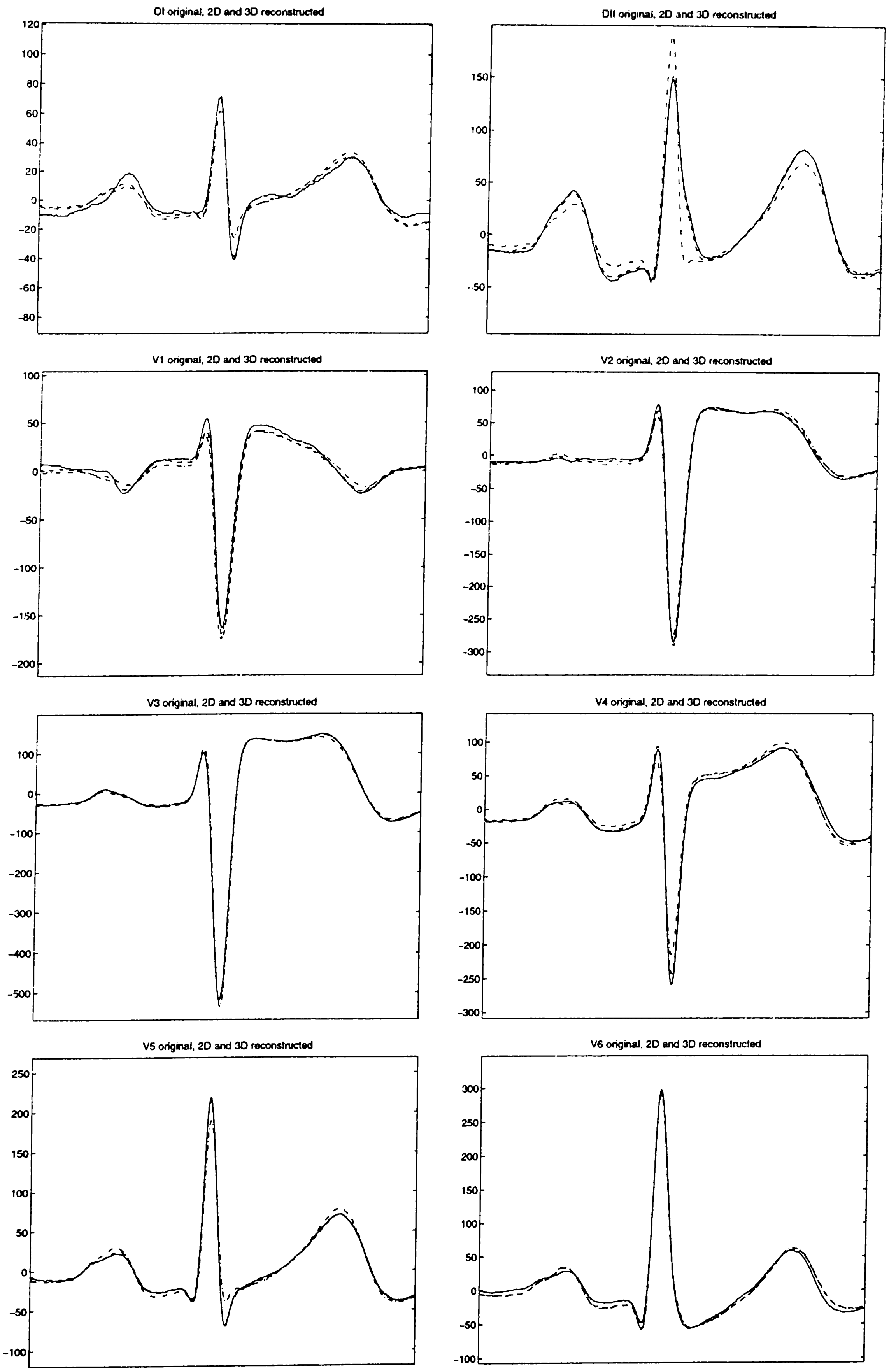

- : input , -. : 2D , - - : 3D

Figure 2.14: 2D versus 3D Reconstruction

$$
\begin{aligned}
w_0 = [0 \quad 0]^T & \qquad \alpha = 0.005 \\
\text{for i} &= 0 \text{ to N} \\
p_i &= w_i^T s_i \\
w_{i+1} &= w_i + 2\alpha(d_i - p_i) R s_{i+1}
\end{aligned}
$$

where p is the predicted signal, w is the vector of coefficients, s is the input signal vector (it is SVD signal channels in our case), d is the desired signal (the original form of the reconstructed signal), R is the estimated autocorrelation matrix of input signals.

Both reconstructions are very close to each other. They differ from the original signal at P and T waves, and at the amplitude of R wave. Such errors can be eliminated by including the 3rd SVD channel in the reconstruction. Since the third channel is not immune to noise as much as the others and since it does not carry significant information about the ST segment much, it is preferred to exclude it. The ST segment of the beat carries the most important information for Exercise ECG Test. Both of the reconstructed beats are almost the same and SVD fits better in V derivations.

The errors made in reconstruction per QRS complex are computed by

$$
\frac{\text{SS of error}}{\text{SS of original QRS}}
$$

$$
\begin{aligned}
\text{SS of error} &= \Sigma_{k=1}^{100} (m_k^{'} - m_k)^2 \\
\text{SS of original QRS} &= \Sigma_{k=1}^{100} m_k^2 \\
m_k^{'} & \quad \text{Sample values of the reconstructed beat} \\
m_k & \quad \text{Sample values of the original beat}
\end{aligned}
$$

The errors in percentage are given in Table 2.2.

In the case of reconstruction of totally lost input channels the most recently used coefficients for that channel before excluding it, are used (see Section 3.1.4). The assumption here is that they do not vary much. This is reasonable since the only high variations are observed in the presence of noise. Whenever dimension is increased, reconstruction coefficients are updated.

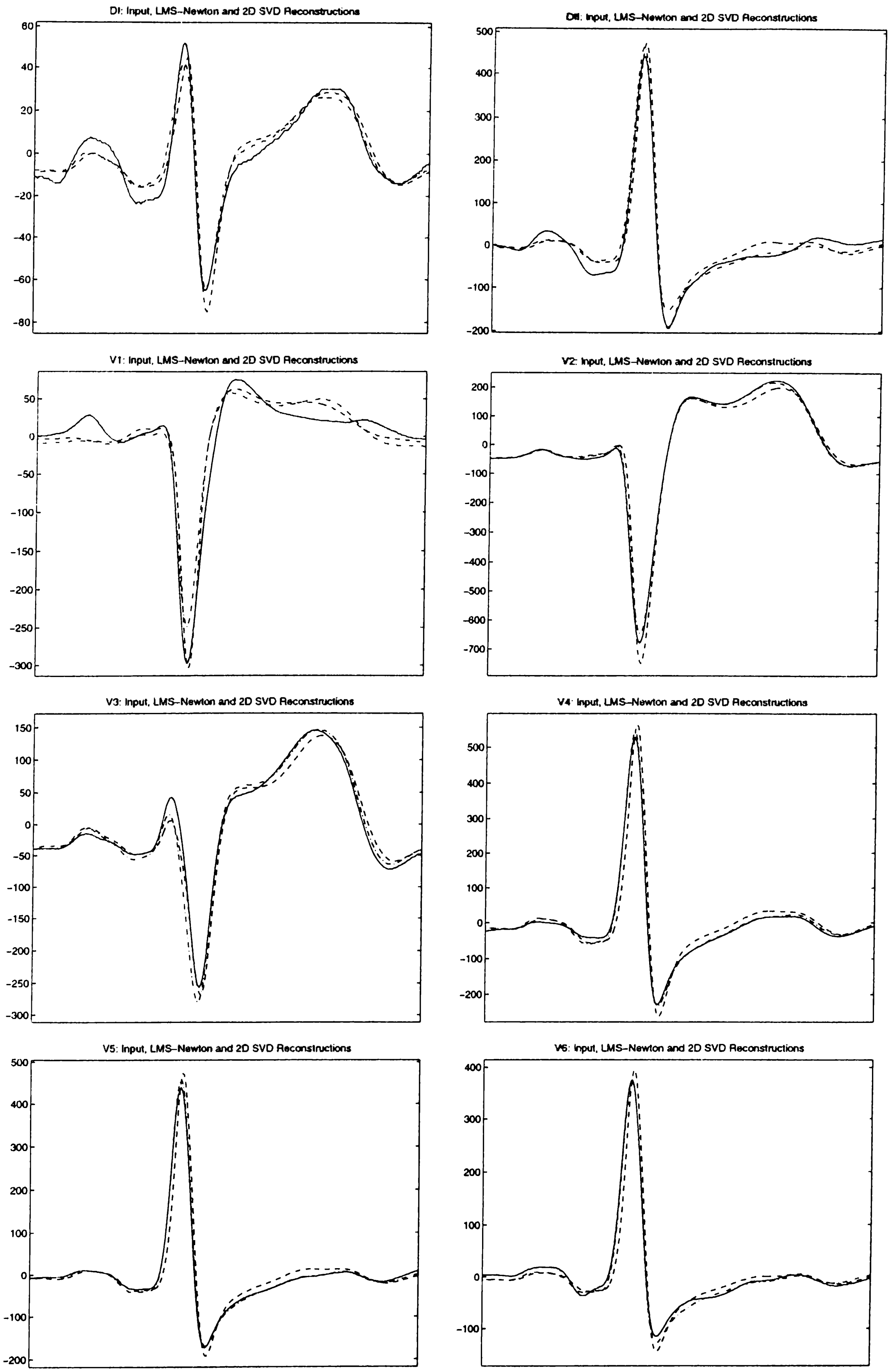

- : input , -. : SVD , - - : LMS-Newton

Figure 2.15: SVD vs LMS-Newton reconstruction

Channel	*Error In SVD Recon.*	*Error In LMS-Newton Recon.*
DI	4.33 %	7.62 %
DII	2.68 %	5.16 %
V1	8.61 %	6.38 %
V2	0.14 %	2.09 %
V3	1.35 %	2.21 %
V4	0.59 %	7.85 %
V5	0.44 %	7.08 %
V6	1.48 %	7.11 %

Table 2.2: Comparison of 2D and LMS-Newton reconstruction errors

2.5 Data Compression

This method improves the compression ratio of ECG signals by eliminating noise.

Compression of information is a direct consequence of eliminating redundancy in ECG signals by orthogonalization. After SVD, all the information can be represented in at most 3 independent channels. This means a compression of at least 3 to 8 without considering reconstruction of standard derivations. Reconstruction is assumed to be a redundant process because if arrhythmia analysis was done using these orthogonal signals, then data compression would be achieved by keeping only the orthogonalized signal set. Such a work was done by Çağlar [16].

Chapter 3

EXPERIMENTS

3.1 Performance On Typical Noise Types

The capability of the algorithm is tested on various noise and artifact contaminated ECG records. Appendix A has examples from these data. Both EMG (Electromyogram) and BW (Baseline Wander) are often observed on DI, which is a channel with low amplitude ECG signal. If such noise , especially BW (low frequency, high amplitude noise), were on DII, a performance degradation is unavoidable due to the special spatial position of DII on the body. Such noise generally interferes with the signal channels at the output of SVD. The algorithm is capable of filtering EMG noise and BW, which are the two basic noise sources in ECG signals. This filtering performance can be reached in even noisy DII cases by taking some precautions like recording DIII independently (see Section 2.3.4). We will also demonstrate the reconstruction of a completely lost input channel from the information in other channels with limited error. Correlations between input channels are instrumental tools in these situations. The reconstruction in such a case uses constant coefficients, so it is not adaptive , however this is the best that can be done in the absence of *desired* (*lost* in this case) signal (LMS algorithms require the desired signal which is the totally lost one in this case).

3.1.1 EMG Noise

EMG noise is a high frequency noise caused by increased muscle activity particularly around the electrodes. Its frequency spectrum is wider than that of

ECG's and overlaps with it. So direct frequency filtering to eliminate EMG distorts ECG signals. Filtering based on moving window averaging does not perform good because biological signals are not stationary. Averaging assumes the noise to be white but this is not always true. It can also distort ECG. These approaches does not make use of the correlations between input channels. Our approach uses the information in other ECG channels to compute the ECG in a noisy channel. Figure 3.1 shows a set of ECG signals with EMG contamination in DI. The decomposed and reconstructed signals are also shown. The EMG in DI is almost completely observable in the noise channels of the decomposed signal set. Reconstruction provides noise-free DI, as shown in detail. The small amount of EMG in DII and V1 is also filtered out. The clean input channels remain unaffected.

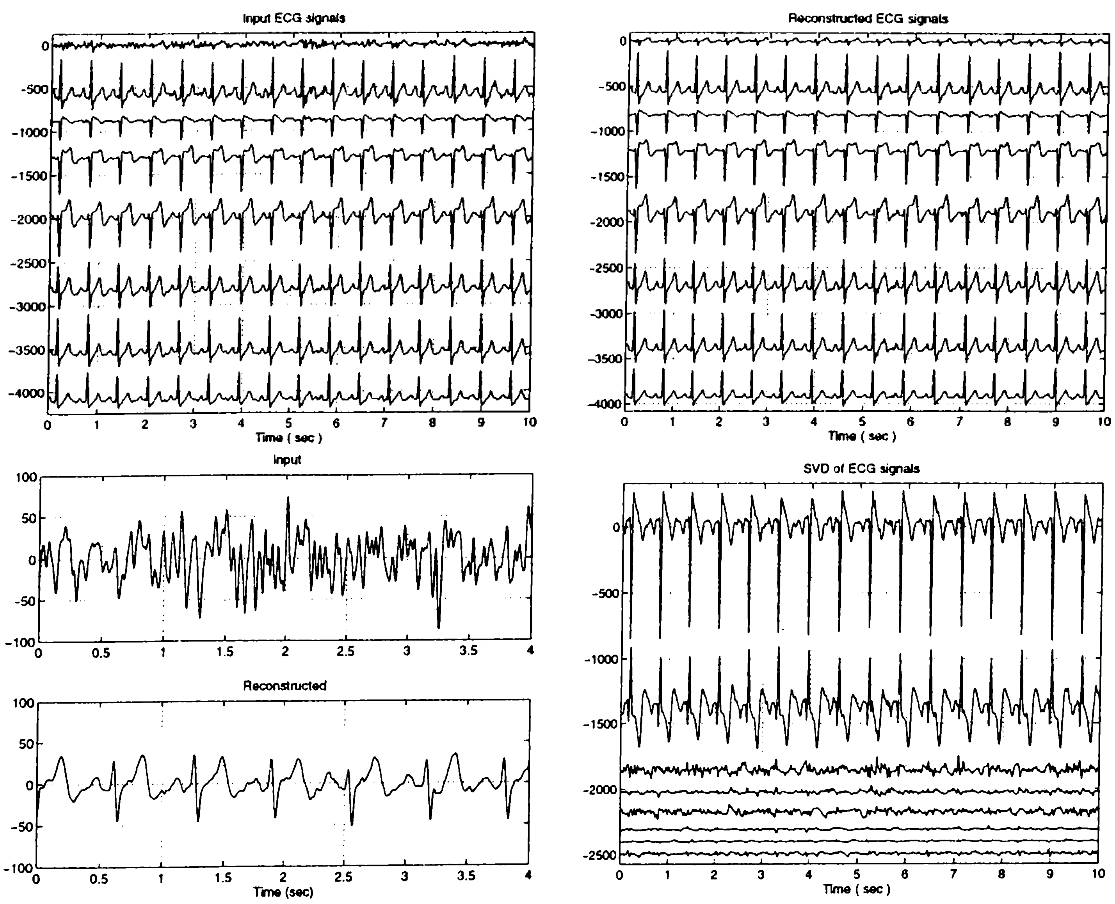

Figure 3.1: ECG with EMG

3.1.2 Baseline Wander (BW)

BW is a low frequency noise caused by respiration and motion of the patient or leads. Its frequency components are usually below 0.5 Hz but during an

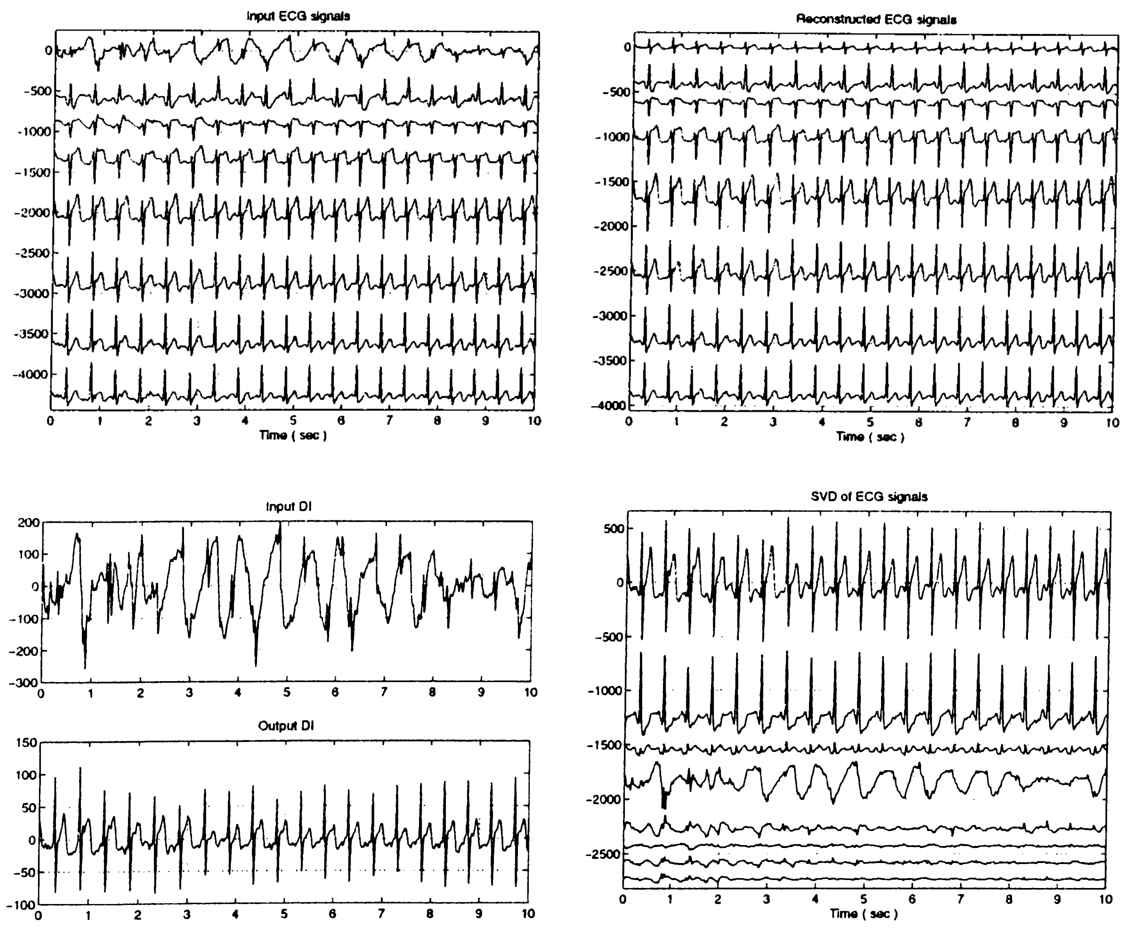

Figure 3.2: ECG with BW

exercise test they extend into the frequency spectrum of ST segments which carry the crucial information in a stress test.

BW has destructive effects after accumulation. It does not rotate the signal vectors significantly during accumulation. It is first represented in noise space. As time passes, the algorithm forgets its past, BW energy accumulates and shifts into the signal space. To avoid this, we either detect accumulation and exclude the noisy input channel and/or enforce a rotation limit to avoid rotation to some extent, on the weakest signal channel (which usually takes BW on). Figure 3.2 is a data with BW on DI. The low energy ECG in the 3rd signal channel is preserved by limiting the rotation of $\mathbf{u}_3$. Thus, BW is completely captured in the noise space. The effects of BW on DII and V1 are also eliminated. These noise components are observable in the 2nd noise channel, i.e. the 5th SVD output channel. Original and reconstructed DI are shown in detail.

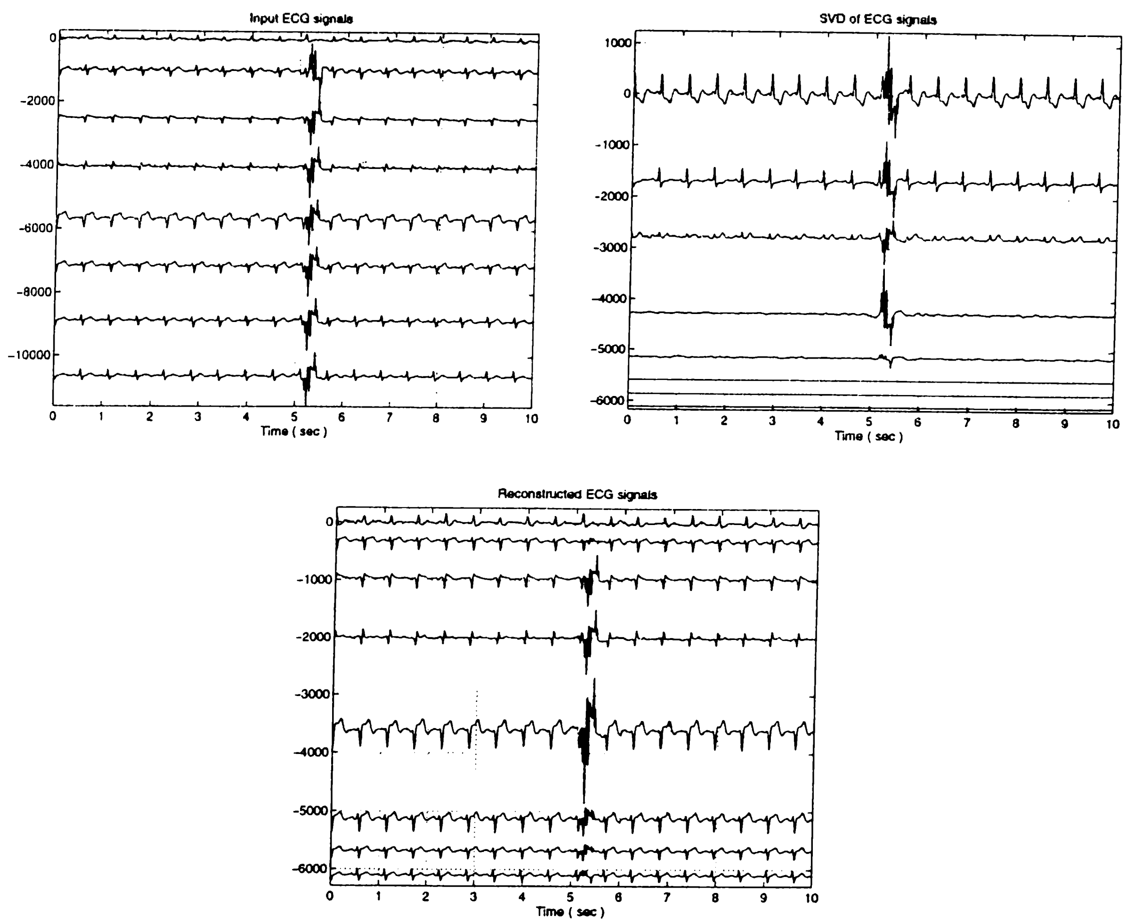

Figure 3.3: Multiple noisy channels

3.1.3 Spikes In All Channels

When a short duration, high amplitude noise arrives from majority of the input channels, vectors rotate and noise channels begin to take on QRS complexes. The implication of this can be in two ways: Either the signal vectors rotate or the QRS complexes in noise channels cause an accumulation alarm. In either case, noise is detected and since it is a multiple noisy input channel case, excluding any one of the input channels is beneficial. If the total noise energy exhibits a steep decrease, over the multiple spike threshold (see Section 2.4.4), then multiple spike alarm is given. If dimension reduction is decided, then the program tries to reduce dimension several times. As a precaution, we recover old **U** and **C** matrices and return to the initial dimension after three noise detections at the same instant, to eliminate the rotation effect. If multiple spike alarm were given, the program would again recover old **U** and **C** matrices to return to the initial dimension. The same thing is done in case of multiple spike detection. In Figure 3.3 a spike shows up in all of the 8 input channels. After detecting the noise, the algorithm excludes 3 of the input channels. Although the rest of the input channels are also contaminated by the noise, they do not rotate the signal space vectors above the threshold. The decrease in dimension results in a decrease in noise energy. DII, V4, V5 and V6 are cleaned almost completely. After the spike has passed, old **U** and **C** matrices are recovered. Dimension reduction more than 3 is not needed. Multiple spike alarm is not given either because that spike is not a very instantaneous one and as a result the decrease in noise energy is not steeper than the threshold.

3.1.4 Totally Lost Input Channel

In some cases, an input channel may be lost completely and only a DC value is read from that lead. This DC value is removed by high pass filtering (see section 2.4.1) and only a constant zero remains. In such cases, this input channel is excluded and is reconstructed from other channels by keeping reconstruction coefficients constant, starting from some time before that channel is lost. This is an erroneous reconstruction because coefficients are not adapted according to the input signal. Part of the error is due to keeping coefficients constant. Part of it is due to the unrecoverable information loss, which is the information contained uniquely in that channel. The reconstruction only uses the related information in other channels, in other words makes use of the correlation between input channels. Figure 3.4 shows the input, decomposed and reconstructed signals of a data set in which there exist EMG in DI and DII, and V2 is lost completely after a high amplitude noise at 3rd second. The EMG noise is observable in the 3rd SVD output channel in the decomposed signal set. V2 is excluded from the input data set by dimension reduction. EMG in DI and DII is also eliminated. Only a small amount of EMG on DII survives. This is due to the special spatial position of DII.

Lost Channel	*Error SS*	*QRS SS*	*Percentage Error*
DI	33	310	10
DII	718	7864	9
V1	351	2317	15
V2	2941	22123	13
V3	639	8204	8
V4	802	13074	6
V5	303	9179	3
V6	461	5973	8

Table 3.1: Table of reconstruction errors

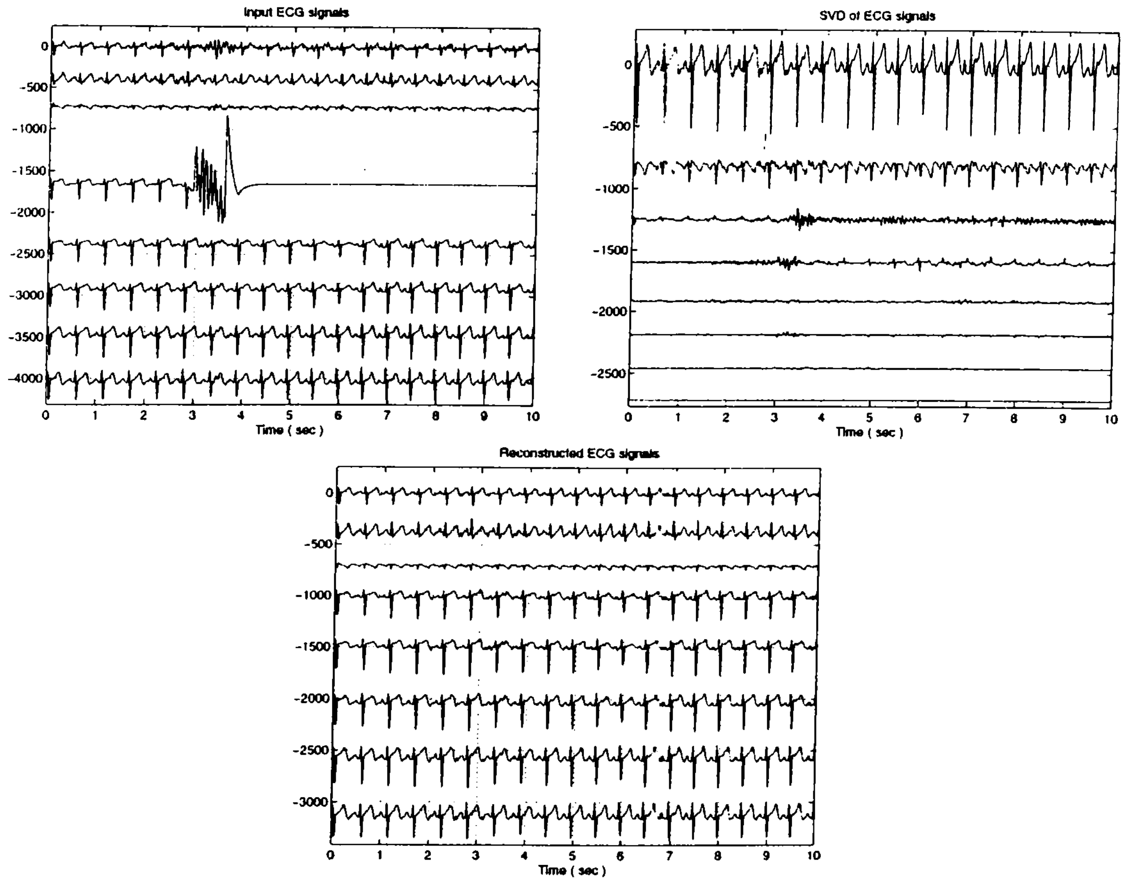

Figure 3.4: Totally lost input channel

Table 3.1 contains the energy of error, in terms of sum of squares, made during reconstruction per QRS complex. Errors are calculated for the beats in Figure 3.5. In this analysis, each channel is made zero manually and then the error between the reconstructed beat and the original beat is calculated as in Section 2.4.8.

Figure 3.5 shows those original and reconstructed QRS complexes from each of 8 input channels.They are obtained by manually excluding the corresponding input channel. ST segment is the most important part of QRS complexes for exercise ECG test and they are reconstructed well for all channels. Only the peaks and especially T wave loses some energy which are not that significant for exercise ECG tests.

3.1.5 ECG With Arrhythmia

The abnormal beats may look like multiple spikes or noise, however, the algorithm does not take them as noise but signal. They are almost completely

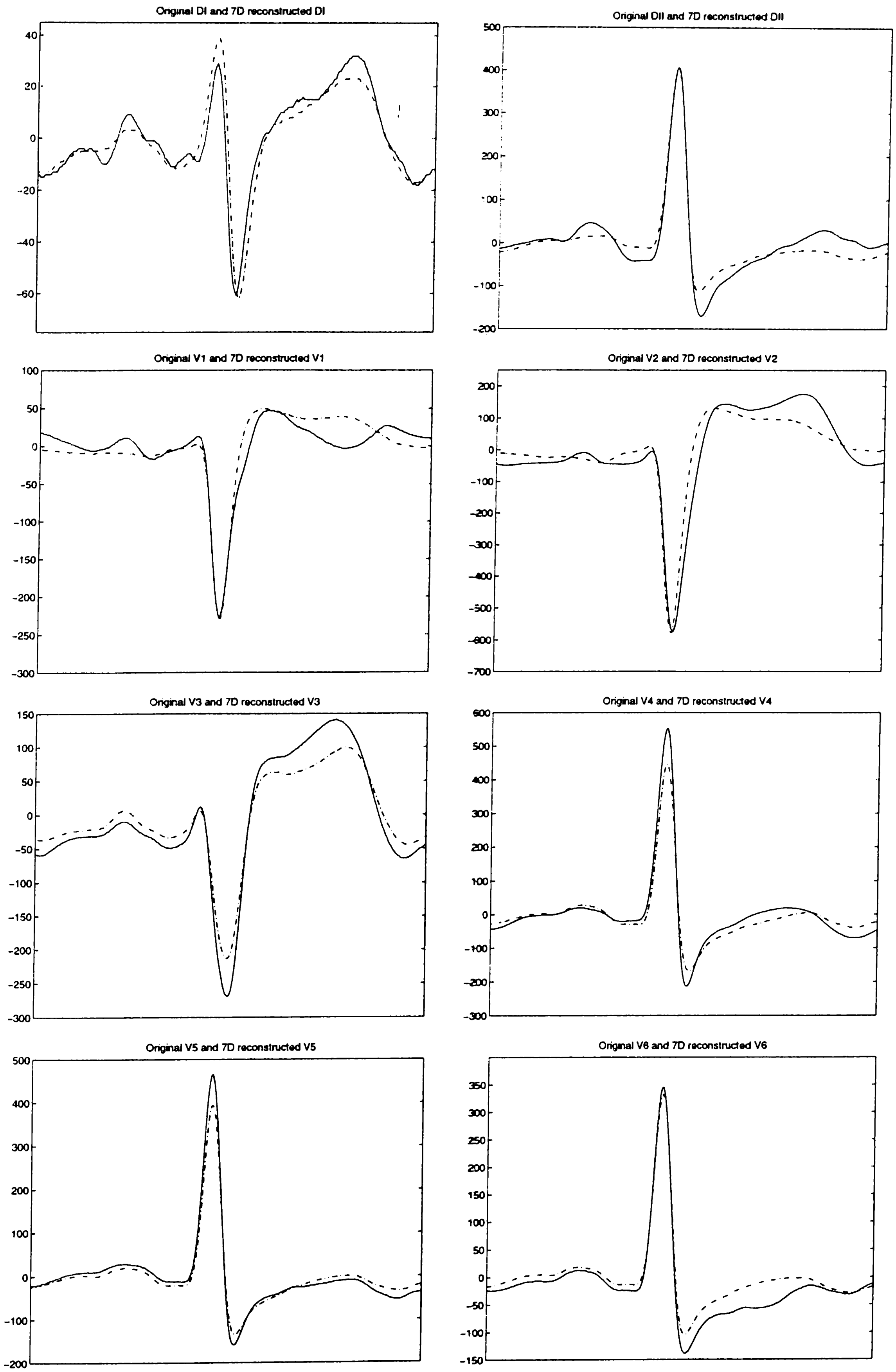

- : Original , -. : Reconstructed

Figure 3.5: Reconstructed QRS complexes during complete loss

represented in the signal space. Figure 3.6 shows a set of noise-free ECG signals with arrhythmia. All of the ECG energy, including the abnormal beats, is observable in the signal space. Only a small portion of the energy of the abnormal beats is taken on by the noise space. As a result, the reconstructed signal set is almost exactly the same as the original signal set. The only difference occurs in the amplitude of the abnormal beats. This loss is due to the small energy in noise channels.

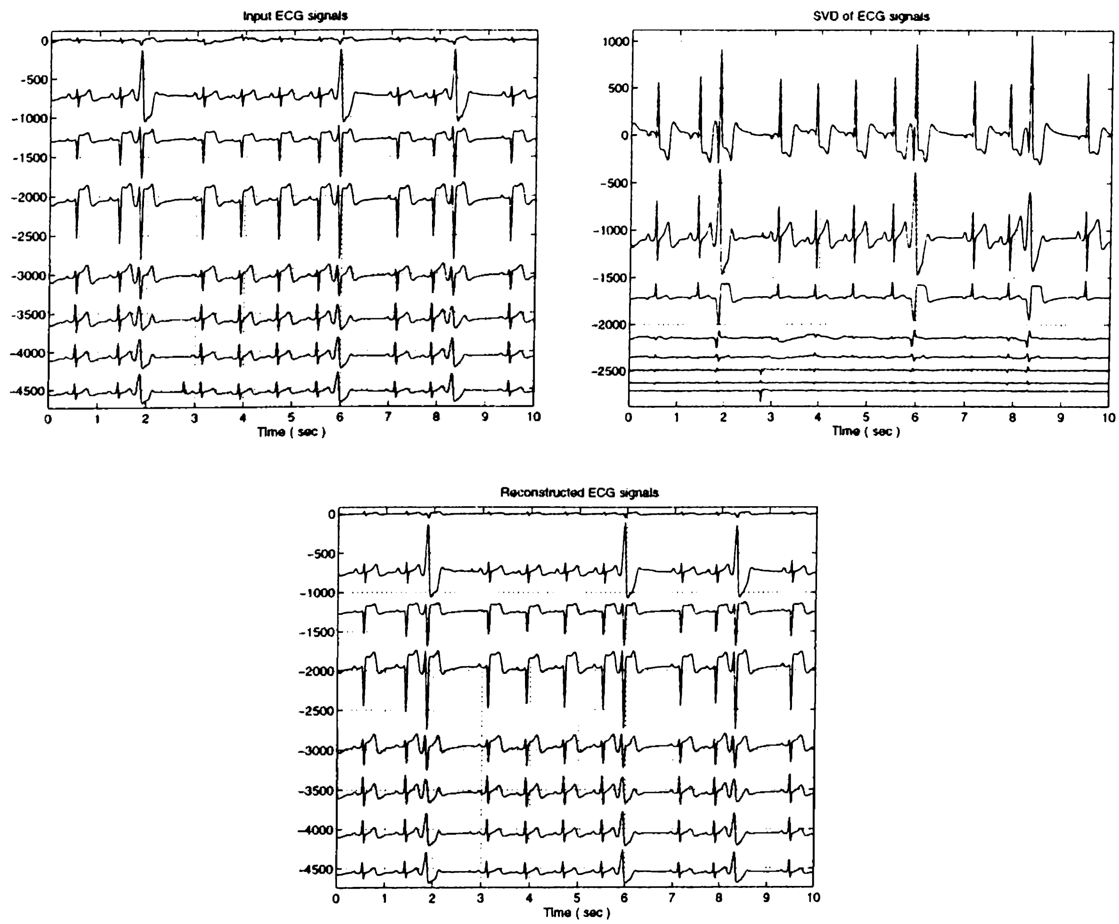

Figure 3.6: ECG with arrhythmia

3.1.6 Correlated BW In All Input Channels

The performance of the algorithm is interesting when a correlated BW in all channels except DI, which is a low energy channel, arrives.

Figure 3.7 shows input, decomposed and reconstructed signals when there is a high amplitude and correlated noise in the majority of the input channels. At first the algorithm tried to eliminate the source of rotation, i.e. noise, by dimension reduction. Since the noise exists in 7 of 8 channels, the algorithm

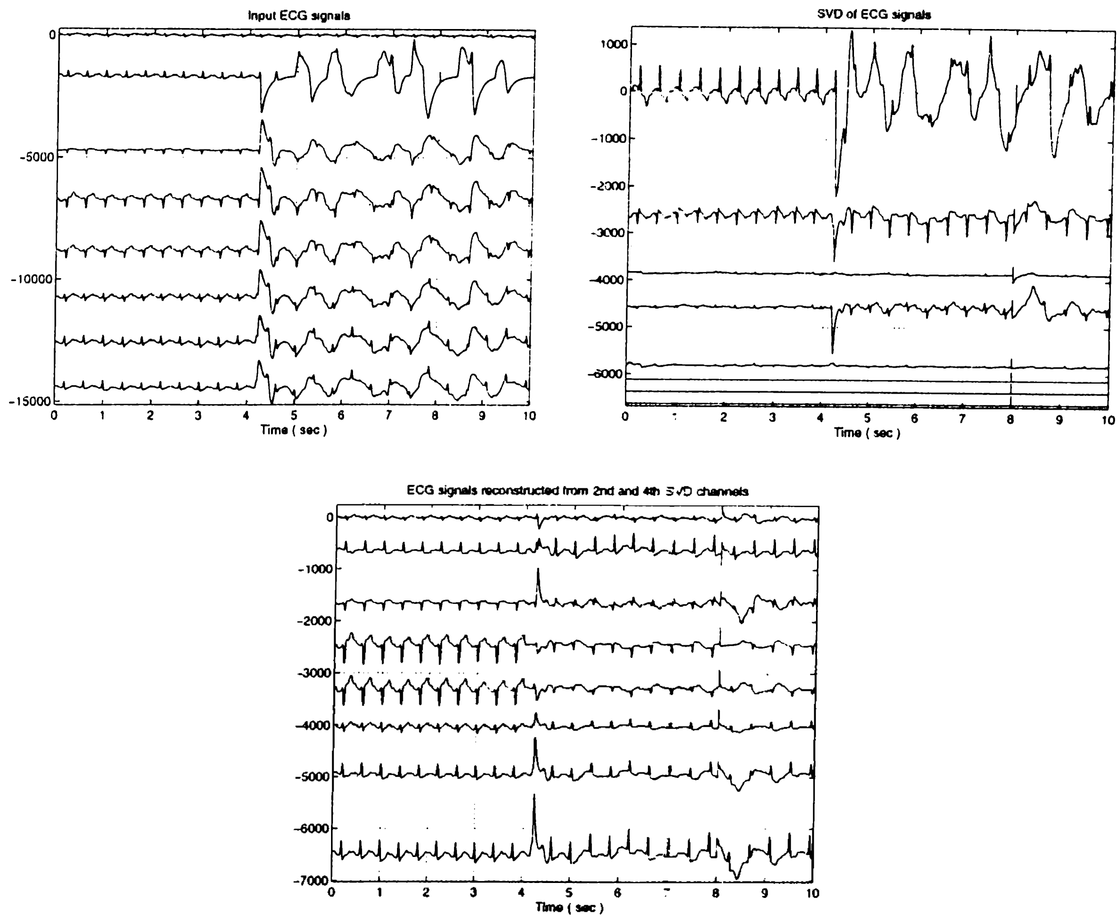

Figure 3.7: ECG with correlated noise

gave up reducing dimension after 3 reductions. Rather the noise is taken as a major signal component and placed, almost completely, in the first SVD channel. The interesting observation made in this data set is that the previously dominant ECG containing SVD output channels are not lost completely. They are shifted to other SVD channels with some noise. Since these channels are used to be treated as noise channels, nothing like rotation limiting or noise detection is applied to these ECG signal containing channels. That is why noise contaminates them. The signal set, reconstructed using these shifted signal channels, are also shown in Figure 3.7. The quality of reconstruction is low because the channels used in reconstruction are treated as noise channels. Another reason for poor reconstruction is that the number of input signal channels was reduced to 5. This also means that constant coefficients are used in the reconstruction of 3 of the input channels. If such a case can be detected and the new signal channels are determined then they can be treated as real signal channels. This would increase the performance of reconstruction.

Appendix B demonstrates the performance of the algorithm when no noise detection is applied to the signal channels. The performance is higher than the one shown in Figure 3.7. The signal channels remain to be noise-free after the shift. They return to their original positions after the noise ends. This shows the potential capacity of the algorithm.

3.2 ST Analysis Results

Many cardiac abnormalities, especially the ones that damage the cardiac muscles, cause some part of the cardiac muscle to stay depolarized all the time. In such cases, a current flows between these abnormally depolarized regions and normally polarized ones. This is called the *current of injury*. The portion of the ECG that is between the end of the QRS complex and the beginning of the T wave is called *ST Segment*. It is important in the detection of current of injury. These currents cause the potential level of the ST segment to shift [14]. This is observable during the Exercise ECG Test.

The ST analysis of the ECG data, obtained from 23 real patients during exercise test, were examined. ECG was recorded with a sampling frequency of 500 samples/sec. ST measurements were done on average beats calculated over successive 20 second episodes. The measurements could be done beat by beat on the outputs of our method but to be able to make a comparison with previous methods, averaging is also applied to the outputs of our method. The highly noisy QRS complexes are excluded from averaging not to affect the average. The number of beats accepted are also recorded to be used as a performance measure of the SVD algorithm. Two measurements were taken at every 20 seconds in all channels. They are taken 60 ms. and 80 ms. after the J point (The exact point at which the wave of depolarization just completes its passage through the heart. It occurs at the very end of QRS complex). Each data set contains the original ECG recorded and the ECG reconstructed using our algorithm.

Rather than the amount of ST segment shift, the trend of these measurements are important, whether they indicate a depression or elevation. The measurements for each of 8 channels of each ECG pair, processed and unprocessed , were compared using *linear regression* by making using of statistical software package, MINITAB (version 8).

The model used is

$$y_i = a \times x_i + b$$

where y_i represents the ST measurements of the original ECG and x_i represents the ST measurements of the processed ECG. The t confidence interval [15] for a is calculated by

$$a \pm (\text{value from } t\text{-table}) \times (\text{estimated standard deviation of } a)$$

t value chosen corresponds to the degrees of freedom for each data set and to 95% confidence.

Figures 3.8 and 3.9 show the comparison of ST measurements, from all channels, belonging to a patient with ST segment level shift. Figures 3.10 and 3.11 belong to a patient with normal ECG. There are 45 and 66 ST measurements in abnormal and normal ECG cases, respectively. The fitted regression lines are also shown. Tables 3.2 and 3.3 show the coefficient a of these regression lines and its confidence intervals.

The slope of the regression lines, when there is ST potential shift, are almost 1. This indicates that the ST measurements taken from the reconstructed signals are essentially same as measurements from raw data. A line cannot be fitted to the data when there is no ST potential level shift because the measurements were gathered in a narrow region. However, the comparison of the measurements shows that they are almost equal.

We must note that ST potential level shifts, when exists, may not be seen in all channels. The fitted regression line is meaningful when the ST measurements are distributed within some range. In all cases, the increase in the number of QRS complexes shows the improvement. For example, the outliner data point in graphs of ST measurements on channel V3, in Figures 3.8 and 3.9, is due to an increase from 11 to 37 accepted QRS complexes. As a result of this increase, ST measurements' trend does not have any discontinuity. That point, shown in Figures 3.8 and 3.9, exhibits a discontinuity in the measurements taken from raw data. That measurement is very different than the other measurements. It is 0.47mV whereas the others range between 0.05mV and 0.25mV for the raw data. The ST measurement at the same time period, on the reconstructed ECG falls in the same range of 0.2mV to 0.4mV with other measurements. This is observable in both ST60 and ST80 measurements.

Channel	*ST 60*		*ST 80*		*QRS1*	*QRS2*
	a	*Confidence Int.*	*a*	*Confidence Int.*		
DI	0.6965	[0.5742,0.8188]	0.8738	[0.7980,0.9496]	1733	1802
DII	0.9133	[0.7742,1.0524]	0.9906	[0.9015,1.0796]	1625	1765
V1	0.7675	[0.5082,1.0268]	0.7600	[0.5312,0.9887]	1776	1809
V2	0.7818	[0.6428,0.9208]	0.9013	[0.7721,1.0305]	1693	1790
V3	0.9123	[0.6439,1.1807]	1.0214	[0.7742,1.2686]	1624	1685
V4	0.9193	[0.8118,1.0267]	1.0146	[0.9302,1.0990]	1676	1692
V5	0.8628	[0.7359,0.9896]	0.9179	[0.8064,1.0294]	1691	1737
V6	0.9388	[0.8161,1.0615]	0.9875	[0.8768,1.0981]	1756	1790

Table 3.2: Table of ST analysis of an abnormal ECG

Channel	*ST 60*		*ST 80*		*QRS1*	*QRS2*
	a	*Confidence Int.*	*a*	*Confidence Int.*		
DI	Regression not meaningful				1137	1168
DII	Regression not meaningful				1004	1058
V1	Regression not meaningful				977	1016
V2	Regression not meaningful				979	999
V3	Regression not meaningful				939	1045
V4	Regression not meaningful				995	1062
V5	Regression not meaningful				1046	1061
V6	Regression not meaningful				1058	1072

Table 3.3: Table of ST analysis of a normal ECG
QRS1 : Number of accepted QRS complexes in the original data
QRS2 : Number of accepted QRS complexes in the reconstructed data

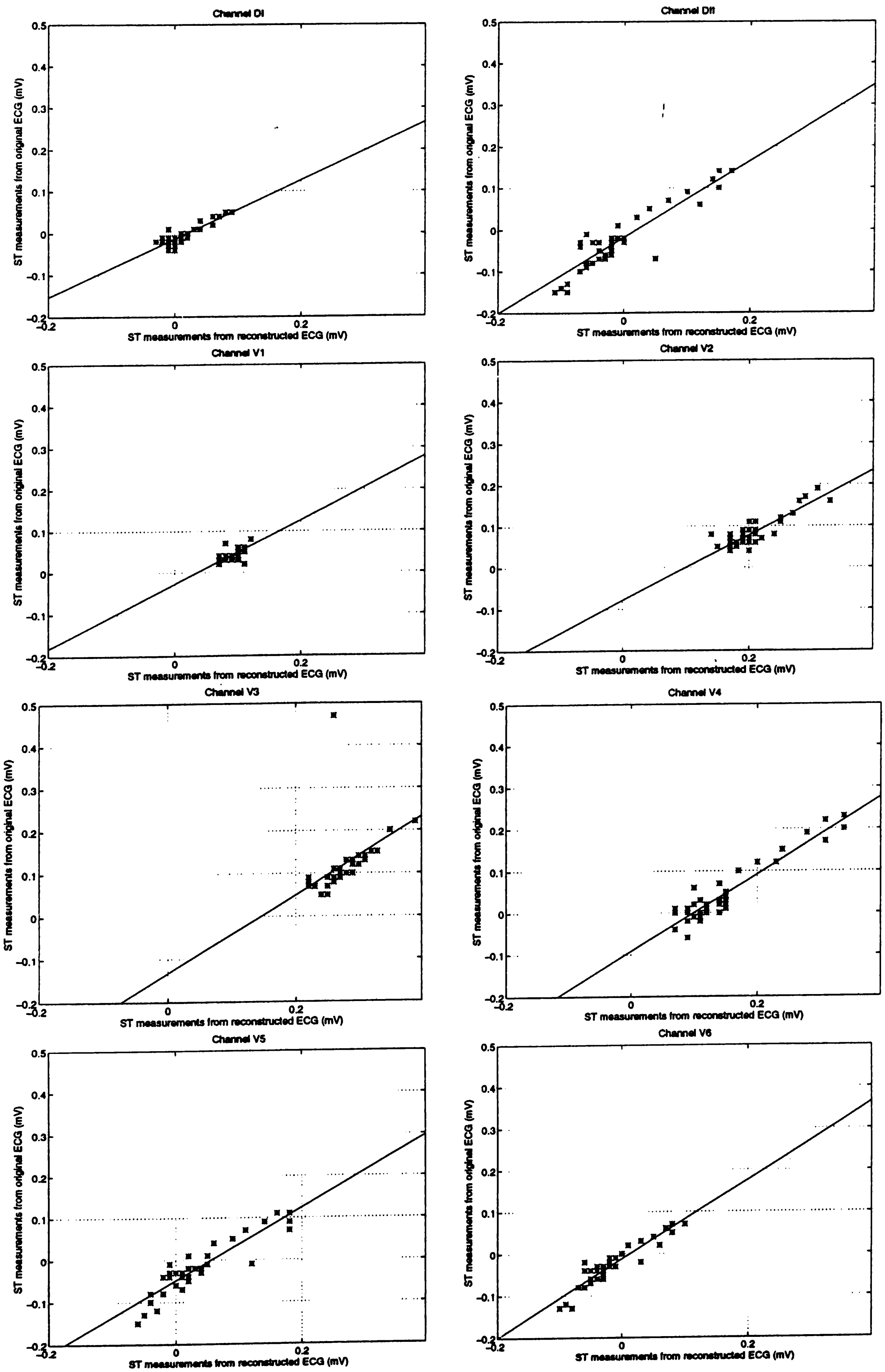

Figure 3.8: Comparison of ST60 measurements of original and reconstructed abnormal ECG signals

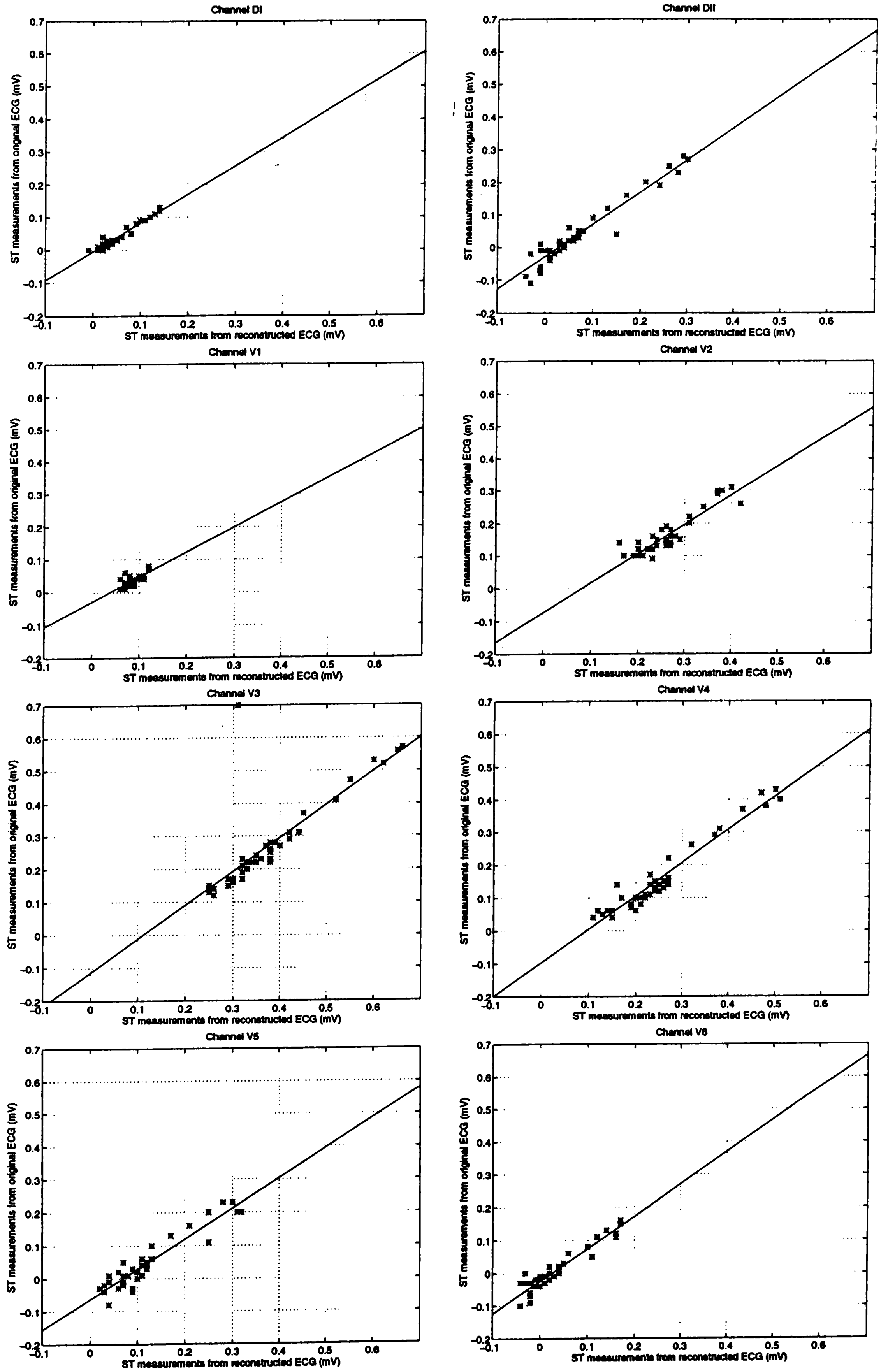

Figure 3.9: Comparison of ST80 measurements of original and reconstructed abnormal ECG signals

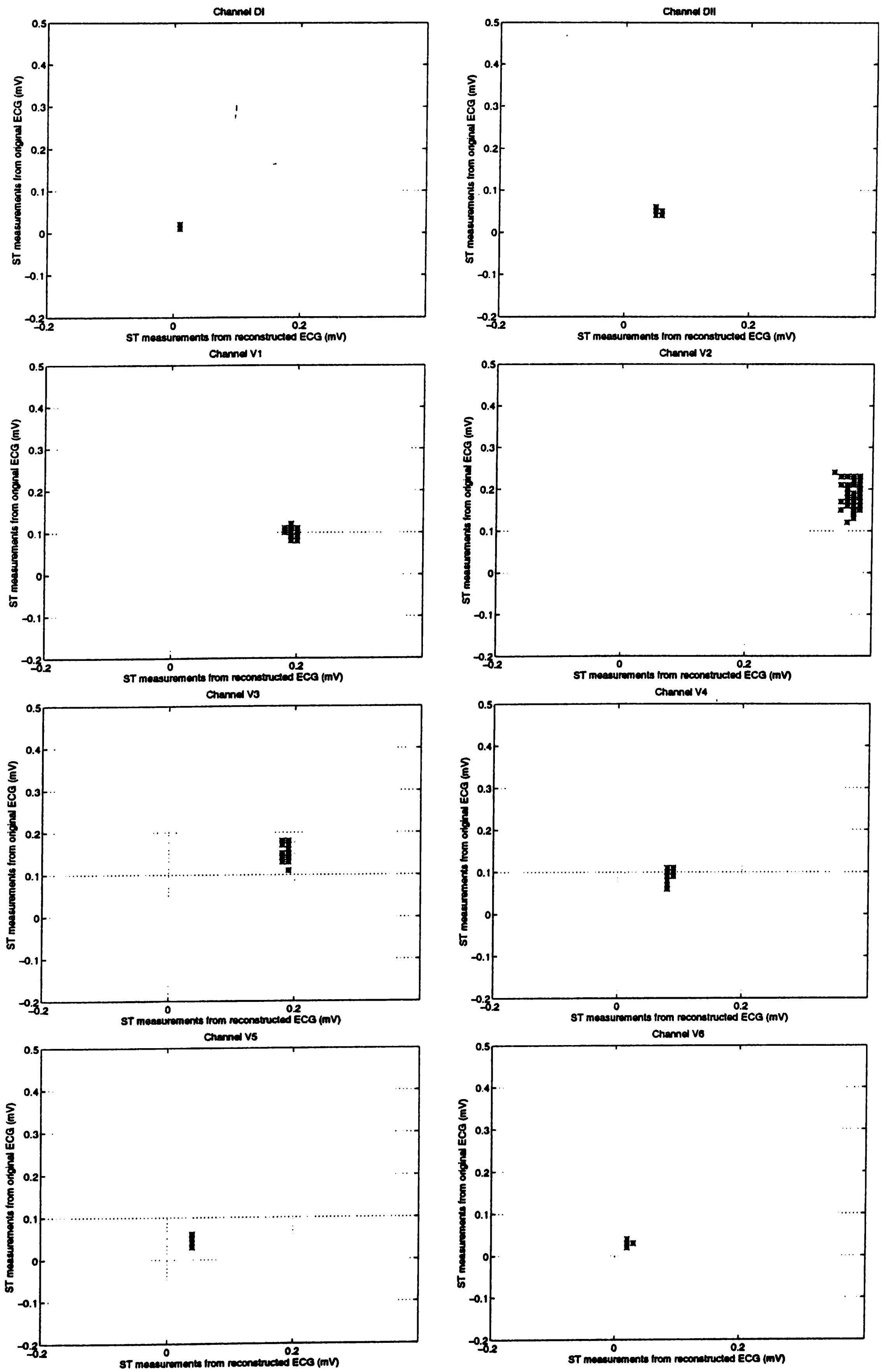

Figure 3.10: Comparison of ST60 measurements of original and reconstructed normal ECG signals

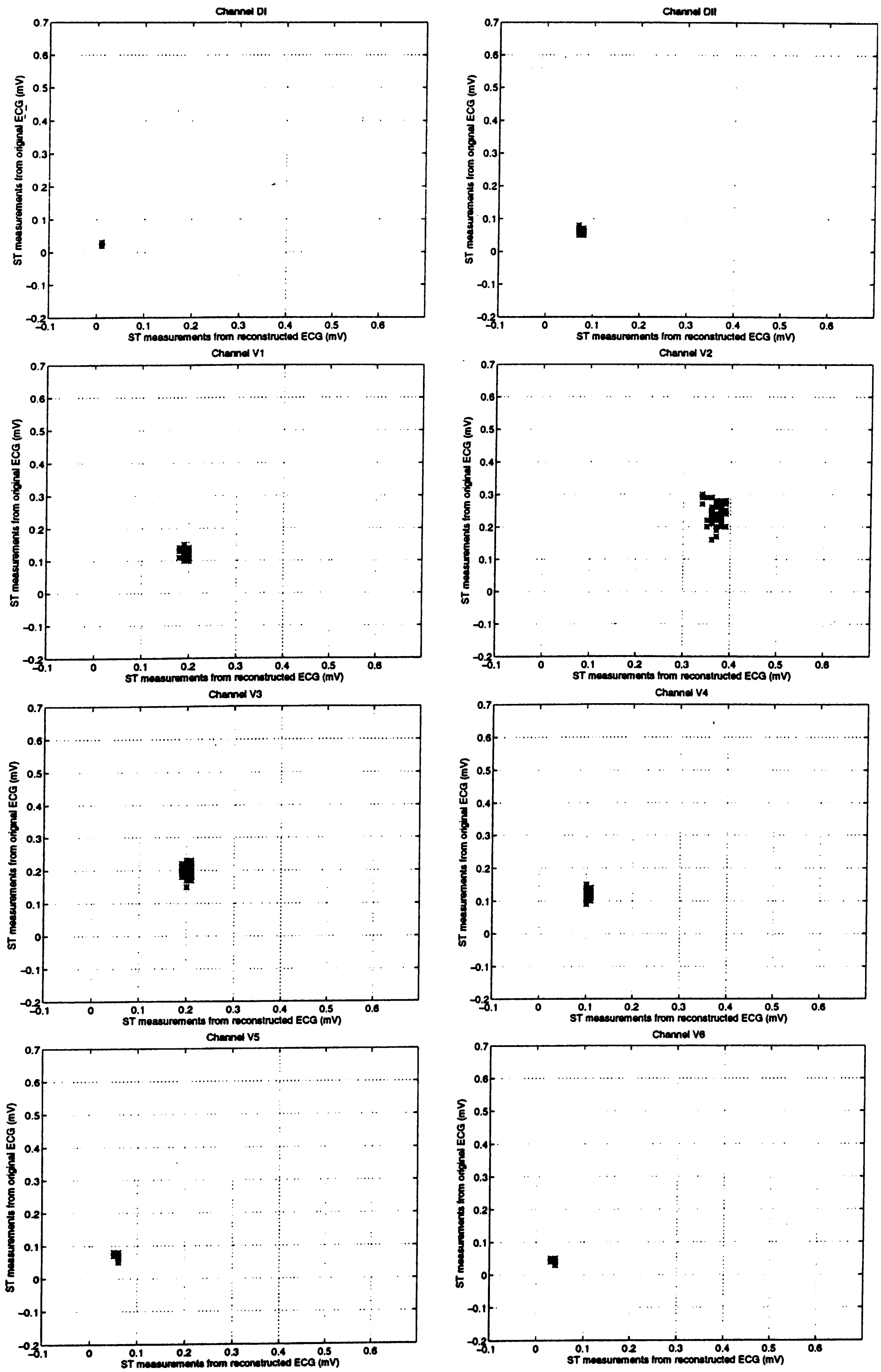

Figure 3.11: Comparison of ST80 measurements of original and reconstructed normal ECG signals

Chapter 4

CONCLUSIONS

A new technique, based on Singular Value Decomposition, was presented in this work. The basic idea is to eliminate the redundancy in standard 12 lead exercise ECG data by orthogonalizing the input signals. Orthogonalization is achieved by removing the dependence between two channels at a time. These channels are selected to be the most correlated two at that instant. The basis vectors, that generate these channels, are rotated accordingly. Since the algorithm is an incremental one, it is adaptive inherently. This adaptive behaviour is used to detect noise and to determine its source. Mainly, rotation of the basis vectors is observed with this aim.

Since 8 of the standard 12 channels are recorded independently, only this set of 8 signals is used. After exhaustive analysis, it became clear that a great portion of the ECG information present in 8 channels can be represented in 2 orthogonal channels. In few cases a 3rd channel also carries information. Noise is mapped to the rest of the orthogonal channels. A reverse operation excluding these noise channels reveals noise-free ECG signals.

The redundancy assures that some part of the information carried in one channel is also present in other channels. This property makes reconstruction of a totally lost channel from the information in others with limited error, possible. The error is limited to the unique information carried on that particular channel. When this is considered, DII is the most unique channel. This is due to its spatial position on the body. Recording DIII would further increase redundancy and decrease the unique dependence on DII.

Different than the previous approaches, SVD based orthogonalization does not disregard any data. Since no averaging or median filtering is applied, all the information present in recorded ECG is preserved in the output signals. The error made in reconstruction is under control. It depends on the number of channels included in the reconstruction. In other words, it depends on the accepted rank of the data matrix. The only possible source of morphological distortion is the HPF applied to remove DC. It does not introduce any significant morphology change. This is assured by the results of ST analysis. However, its minor effect can be avoided by reverse operation of HPF after the reconstruction.

A non-stop exercise ECG test is possible with this technique. This is important because in many cases this test is needed to be repeated due to the failure of recording leads or cables. However, cardiac patients cannot be put under such stress frequently.

Further research is needed to improve the algorithm. One of the problems is the slow accumulation of noise. This cannot be detected by observing the rotations of the vectors. Accumulation check is done, but noise detection via observation of the vectors is a more secure method. Moreover, slowly accumulating noises have low amplitudes. They do not cause any problem for some time, until the accumulation gets high. This means that the algorithm can separate these noises for some time. Some precautions can be taken to maintain this property. The algorithm can be made to separate these noises for longer times by increasing α. The drawback in increasing α is the sacrifice from adaptivity of the algorithm. Further research is needed to find out new methods to overcome this problem.

The specific information content of the orthogonal output channels is another thing to be investigated. If we know what kind of morphological information they carry, we can understand the ECG information disregarded by excluding an orthogonal channel from the reconstruction. At the moment, we know the amount of ECG energy disregarded.

The effect of the reconstruction on the subtle points, like the J point, is also very important. The locations of these points are important because the measurements are done with respect to them. Further research is needed to find out the efficiency of the algorithm in mapping these points.

The algorithm is implemented in Borland C++ under Windows 3.1. More efficient implementations under DOS would further increase the speed of the program. This would allow more comprehensive analysis to be done online on the orthogonalized signals.

The ECG analysis algorithms, which were designed for standard 12 lead ECG records can be modified to work on the orthogonalized signals. These orthogonalized signals carry all the ECG information present in the standard derivations. Thus, there would be no need for reconstruction. Storing the orthogonal signal channels would save storage capacity significantly. As a first step, QRS detection algorithms were applied on these orthogonal signals by Çağlar [16].

Appendix A

Results From The Data Sets Used

This appendix includes input, decomposed and reconstructed signal samples from the data sets used. The noisy parts, if exist, are selected to demonstrate the performance.

The data were recorded with a sampling frequency of 500 samples/sec. under Bruce Protocol. Each sample value was quantized with a 12-bit A/D converter with a swing of 12 mV. The length of data sets range from 9:00 min. to 21:20 min. The order of the channels in each graphic is DI, DII, V1, V2, V3, V4, V5, V6.

Under each column, the number of orthogonal channels used in reconstruction and the indices of the input channels excluded from the decomposition are given.

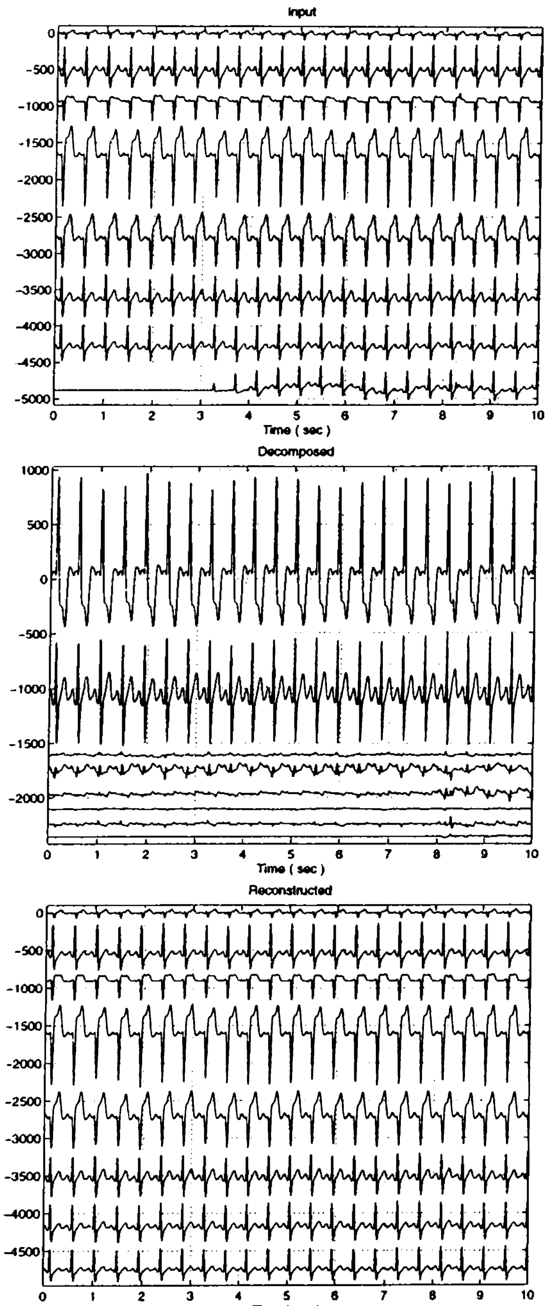

Reconstruction dim.: 2
Excluded channels: No

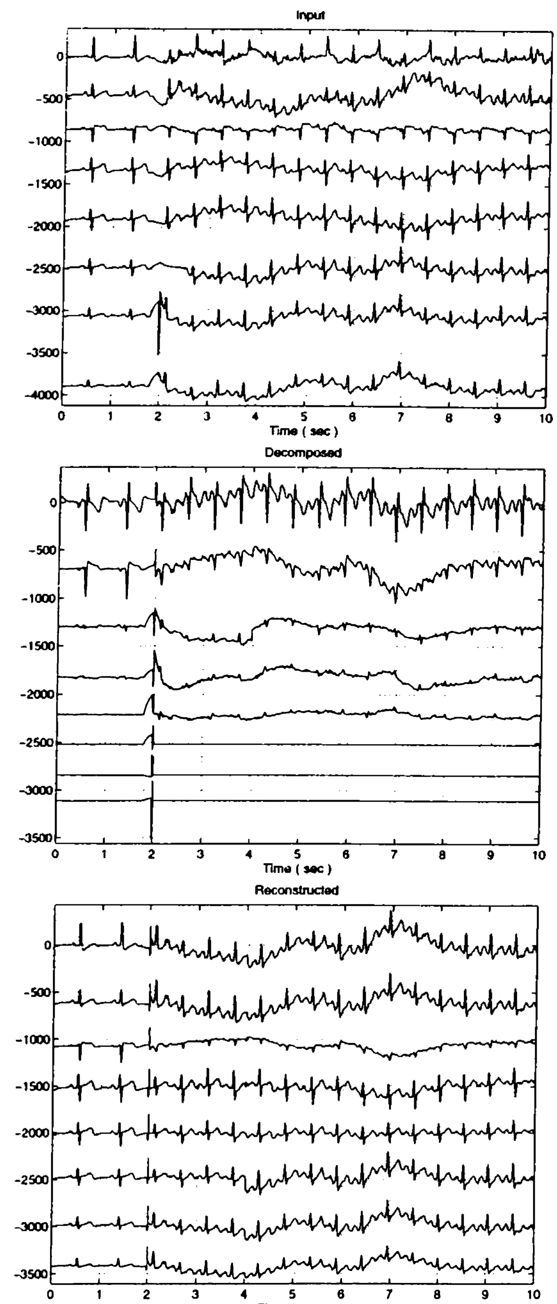

Reconstruction dim.: 2
Excluded channels: No

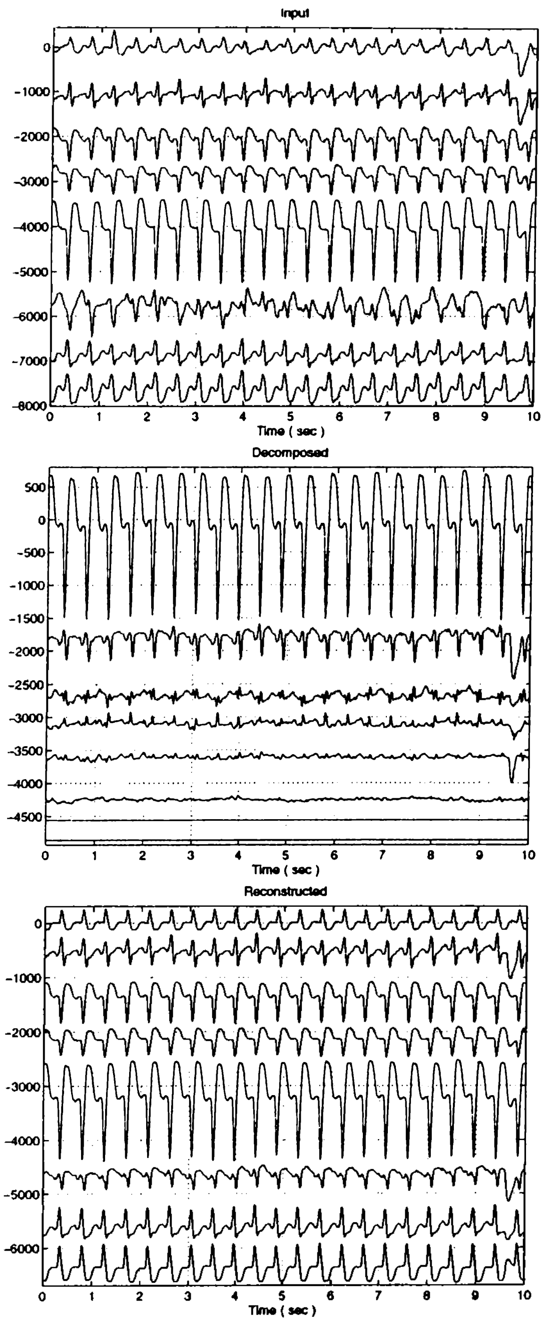

Reconstruction dim.: 2

Excluded channels : 2,6

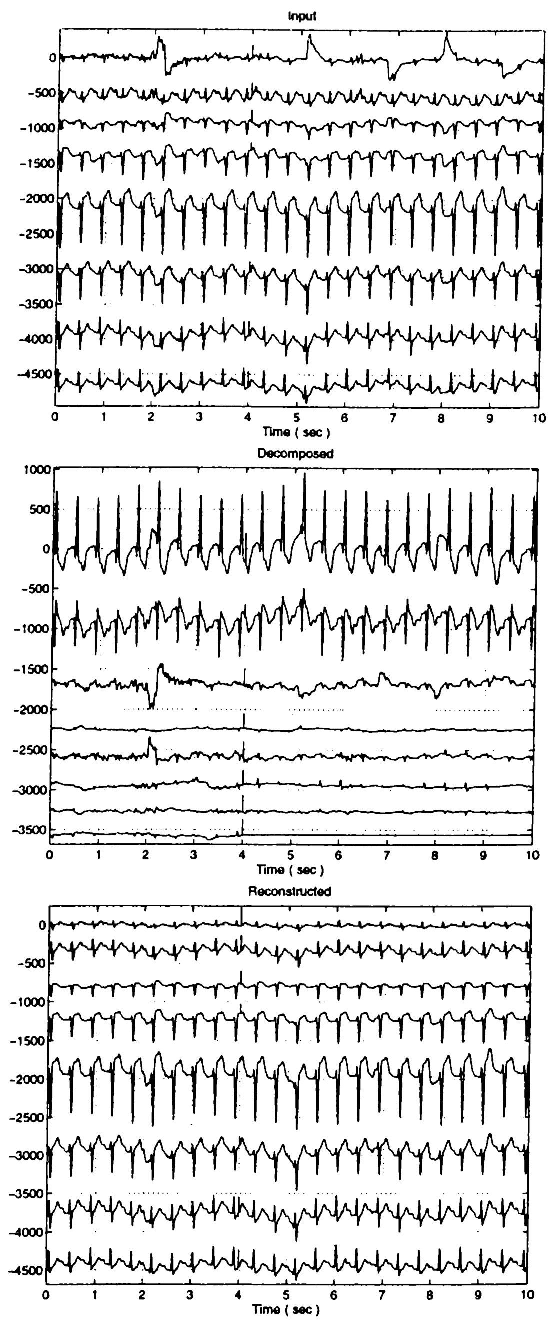

Reconstruction dim.: 2

Excluded channels : 1 after 4th sec.

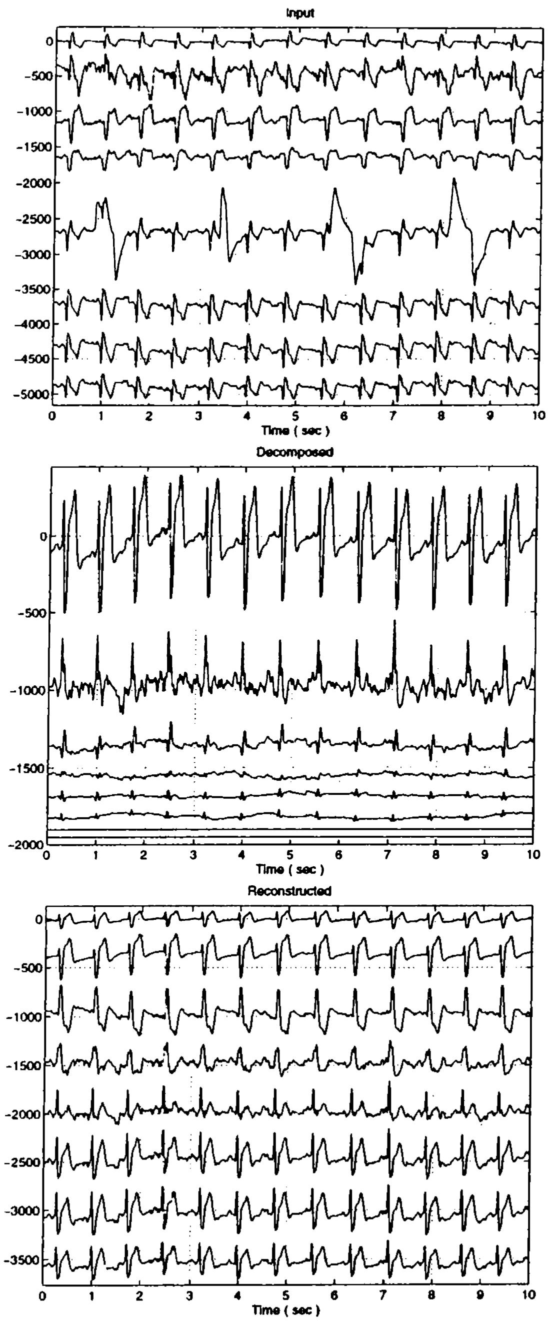

Reconstruction dim.: 2

Excluded channels : 2,5

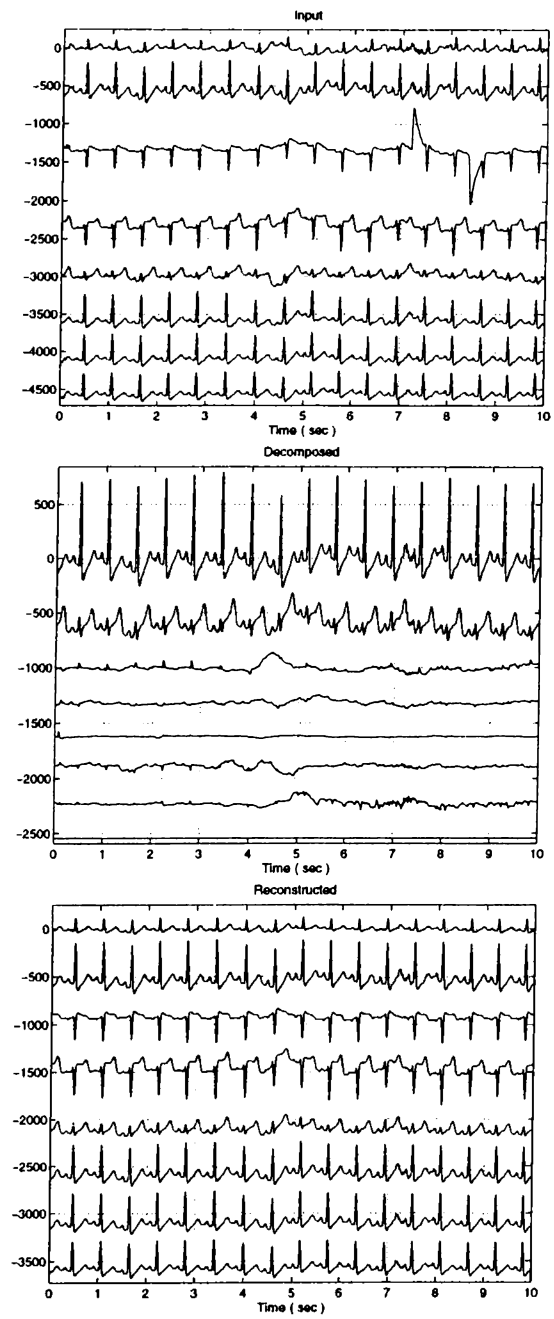

Reconstruction dim.: 2

Excluded channels : 3

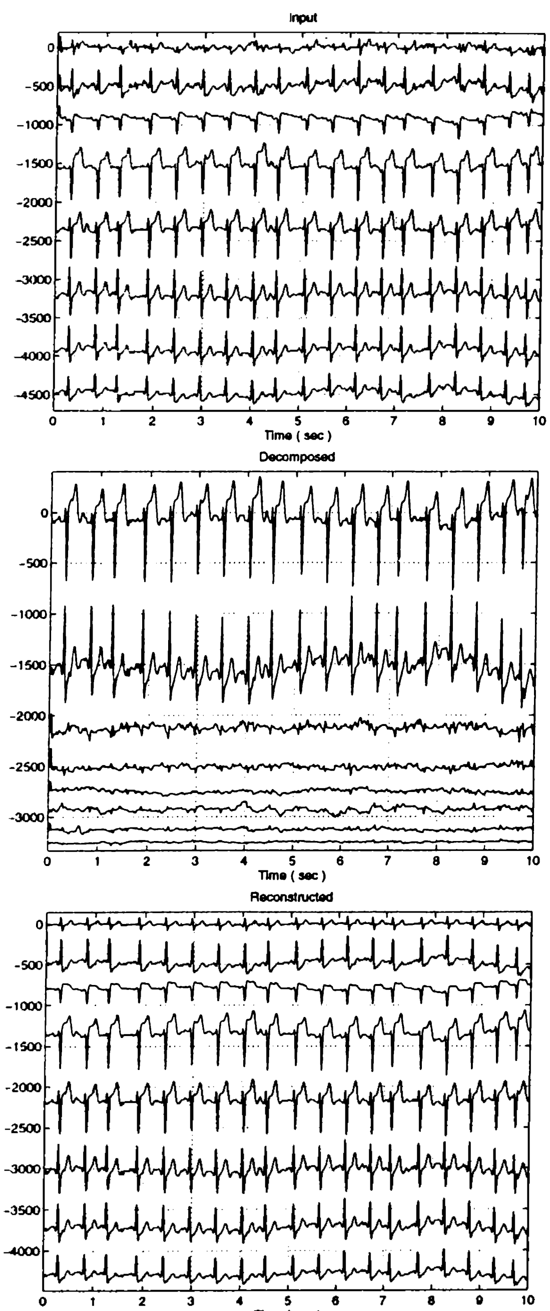

Reconstruction dim.: 2

Excluded channels : No

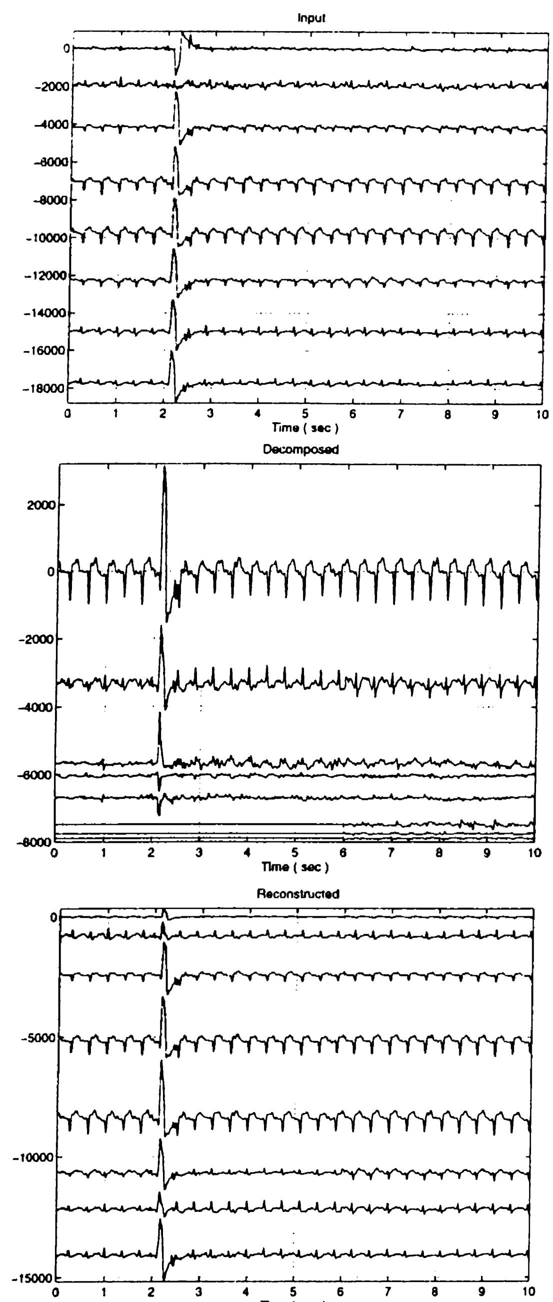

Reconstruction dim.: 2

Excluded channels: 1,5,6 until 6th sec.

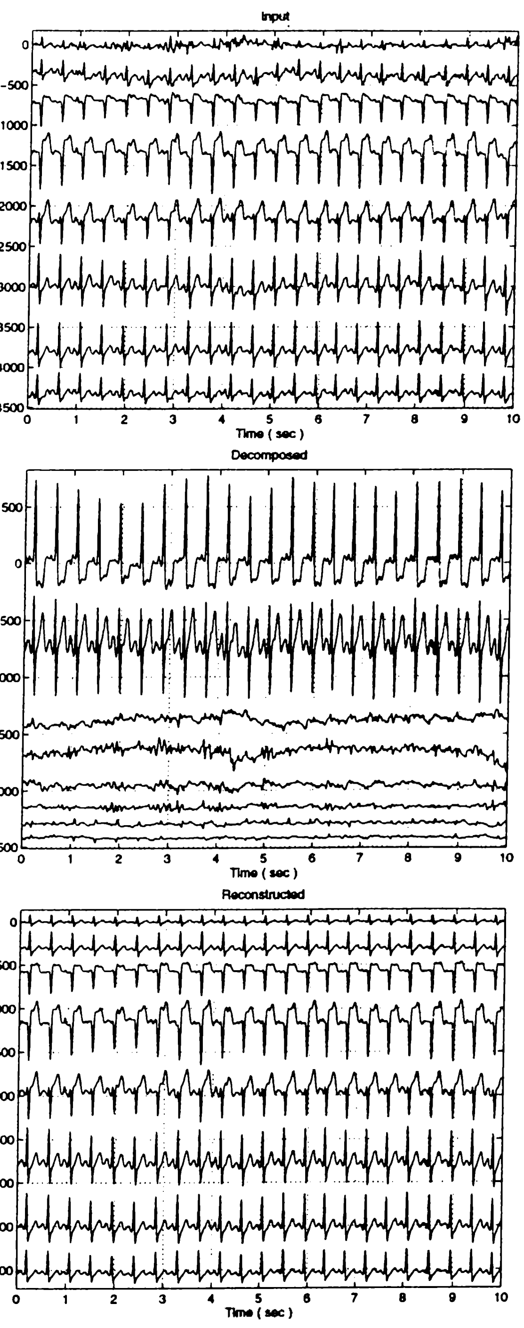

Reconstruction dim.: 2

Excluded channels : No

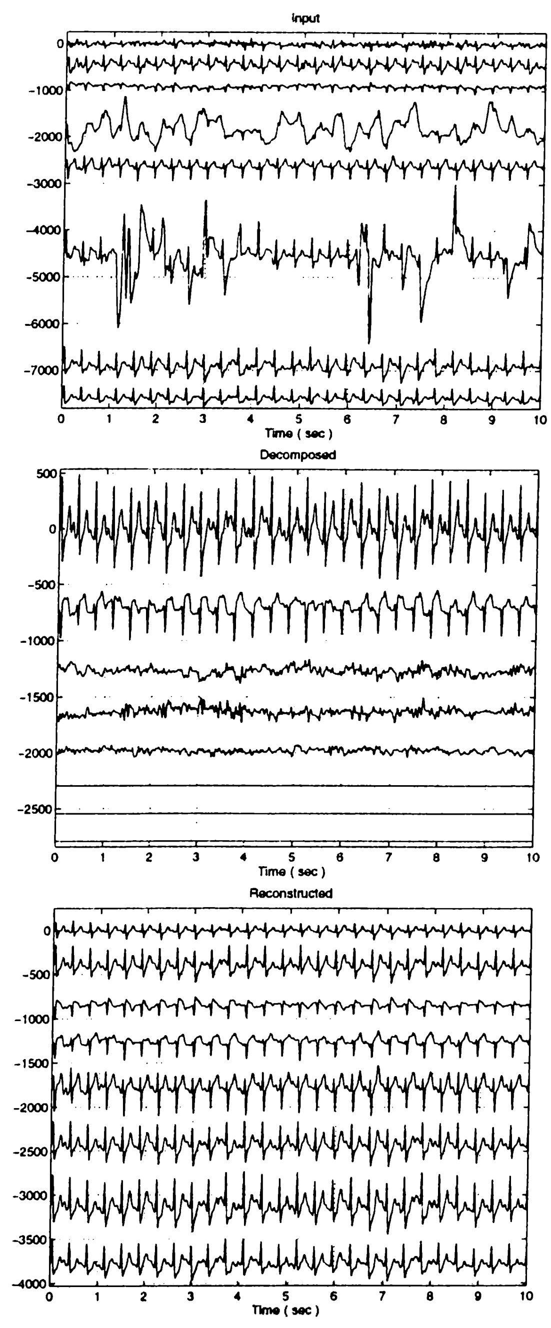

Reconstruction dim.: 2

Excluded channels : 1,4,6

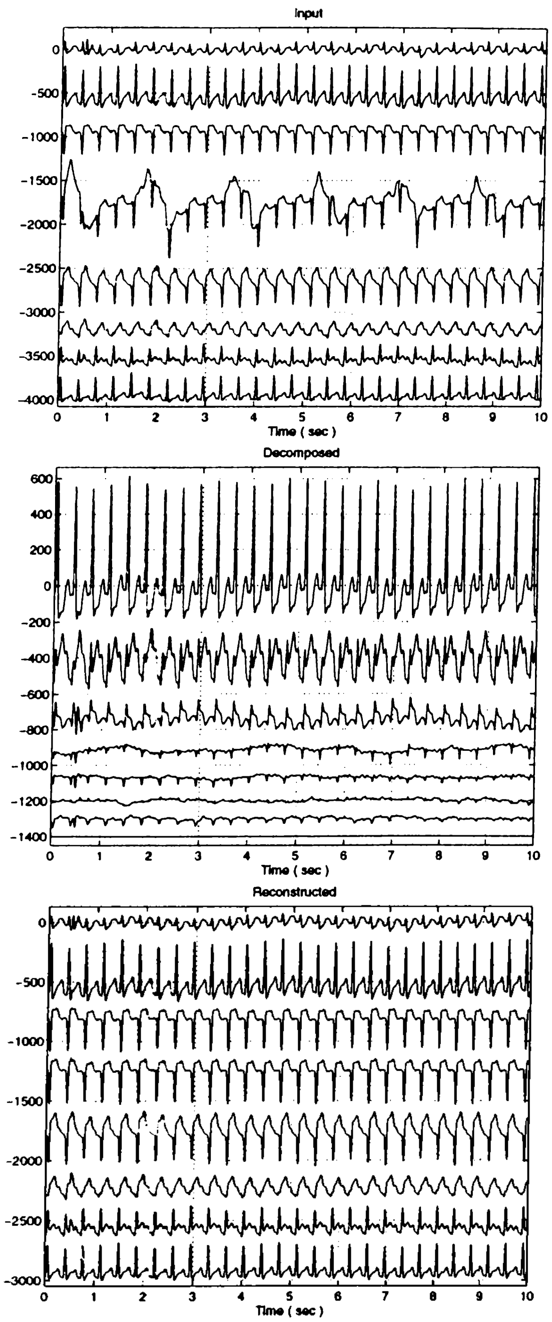

Reconstruction dim.: 3
Excluded channels : 4

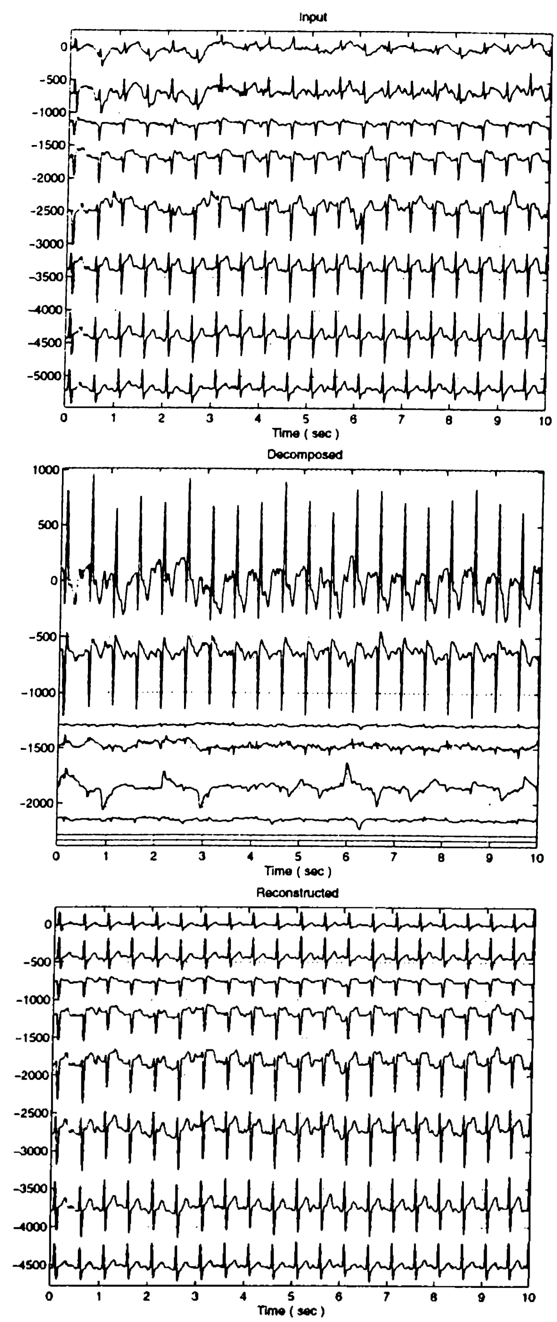

Reconstruction dim.: 2
Excluded channels : 5,2

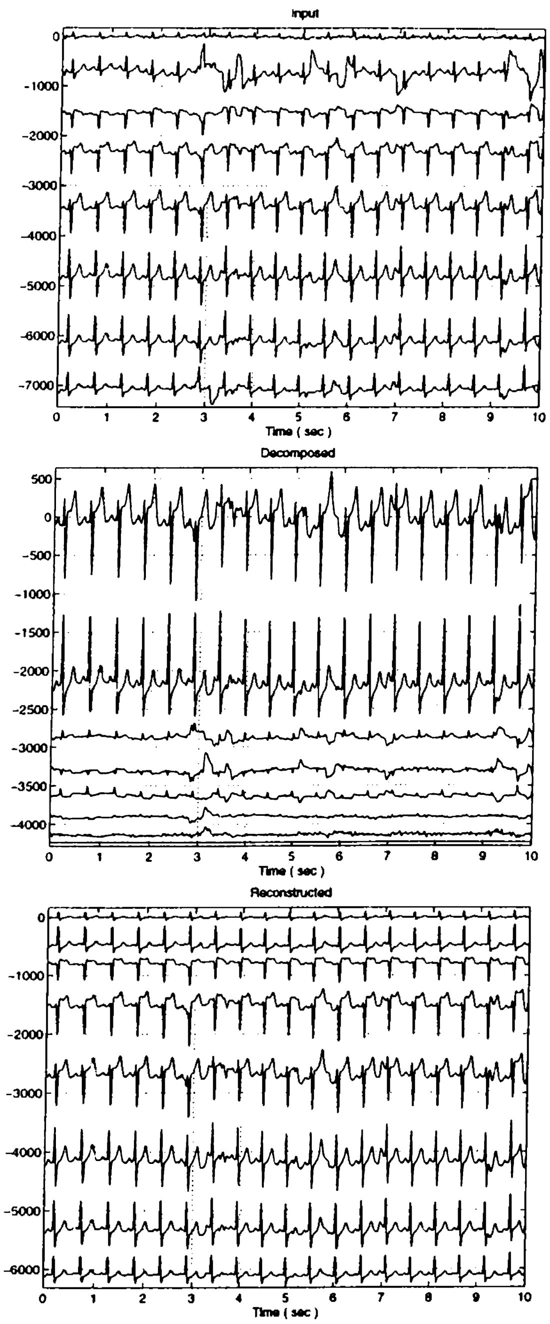

Reconstruction dim.: 2

Excluded channels : 2

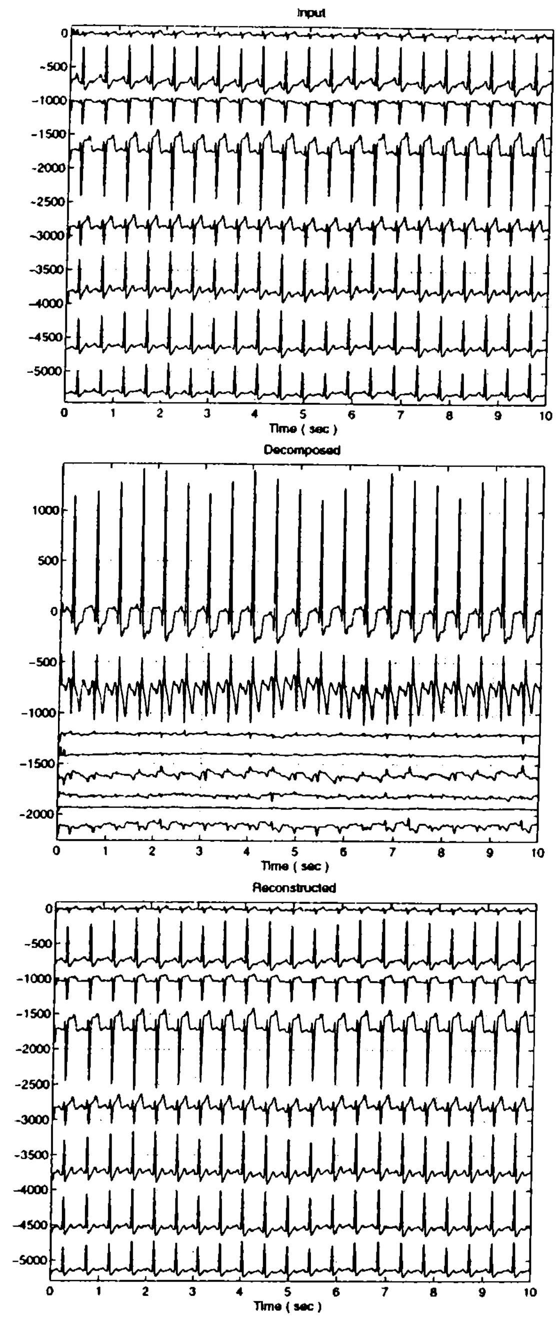

Reconstruction dim.: 2

Excluded channels : No

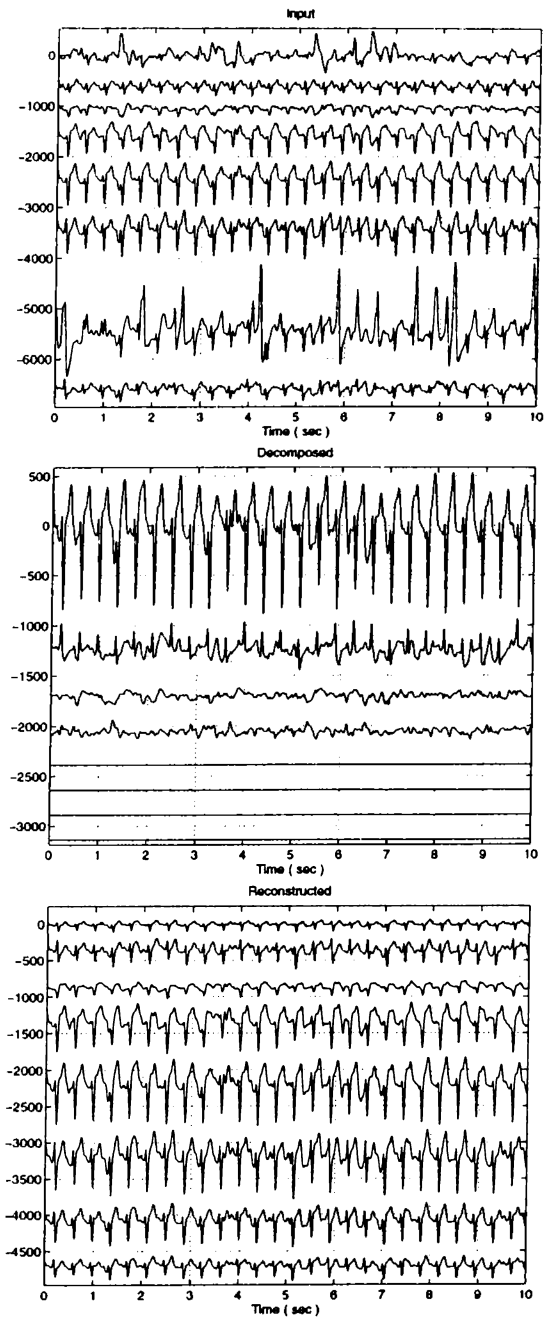

Reconstruction dim.: 2

Excluded channels : 1,5,6,7

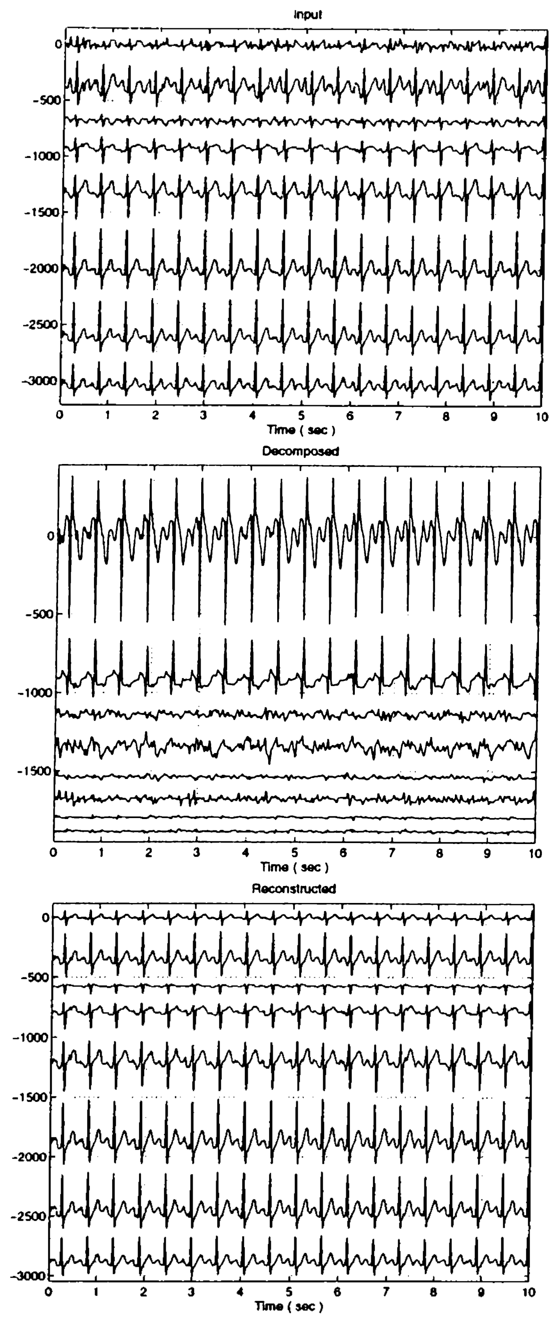

Reconstruction dim.: 2

Excluded channels : No

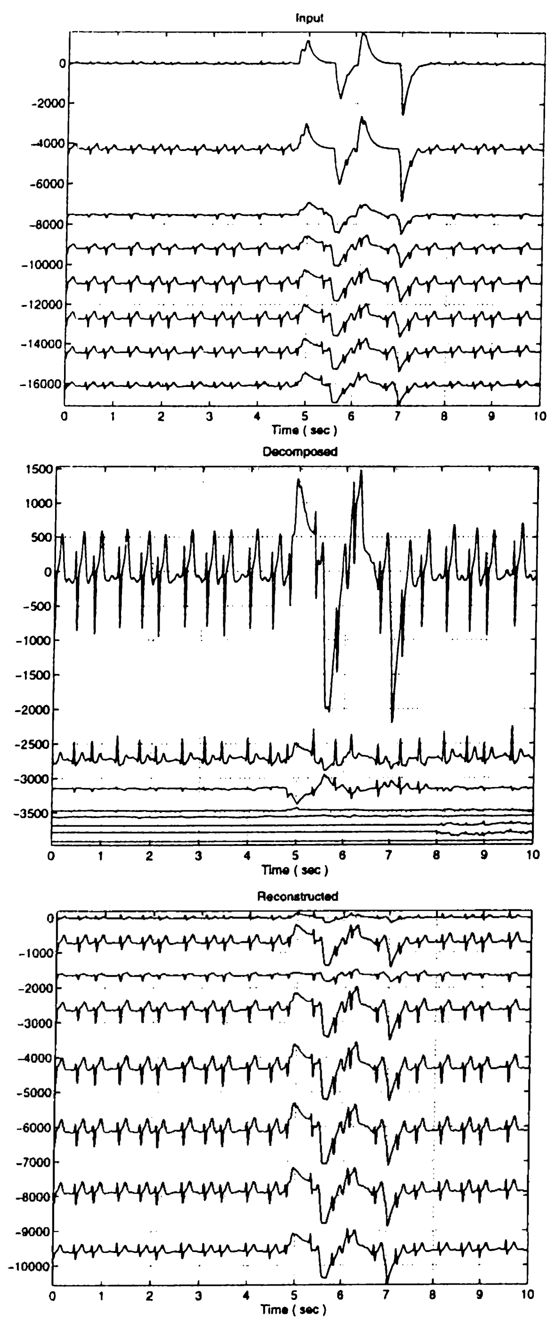

Reconstruction dim.: 2

Excluded channels : 1,2,8 until 8th sec.

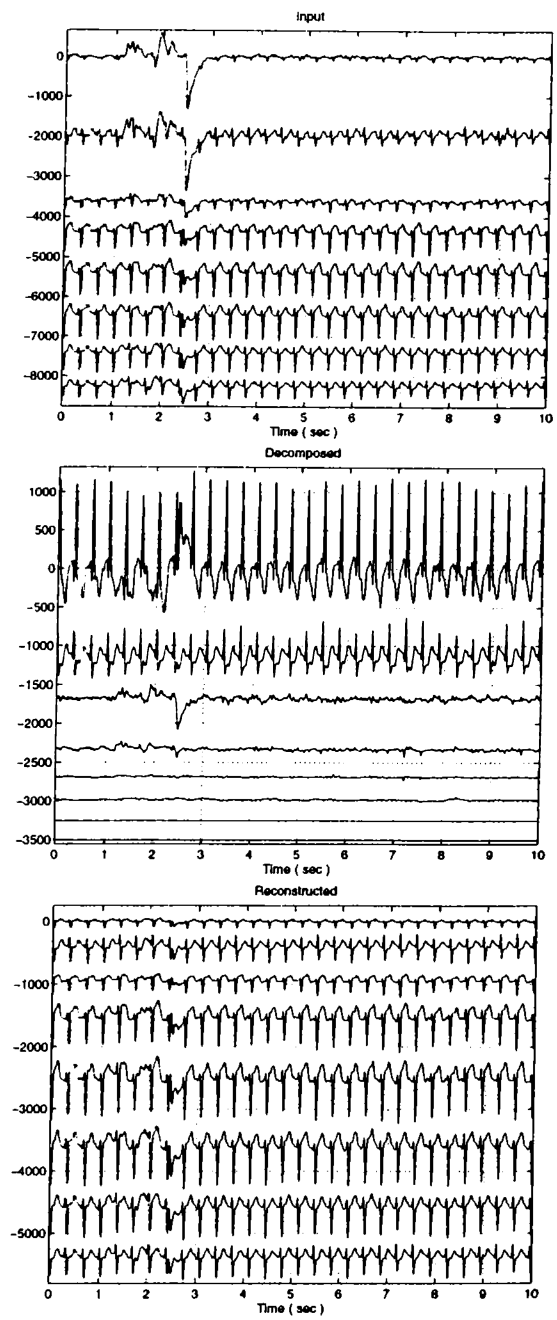

Reconstruction dim.: 2

Excluded channels : 1,2

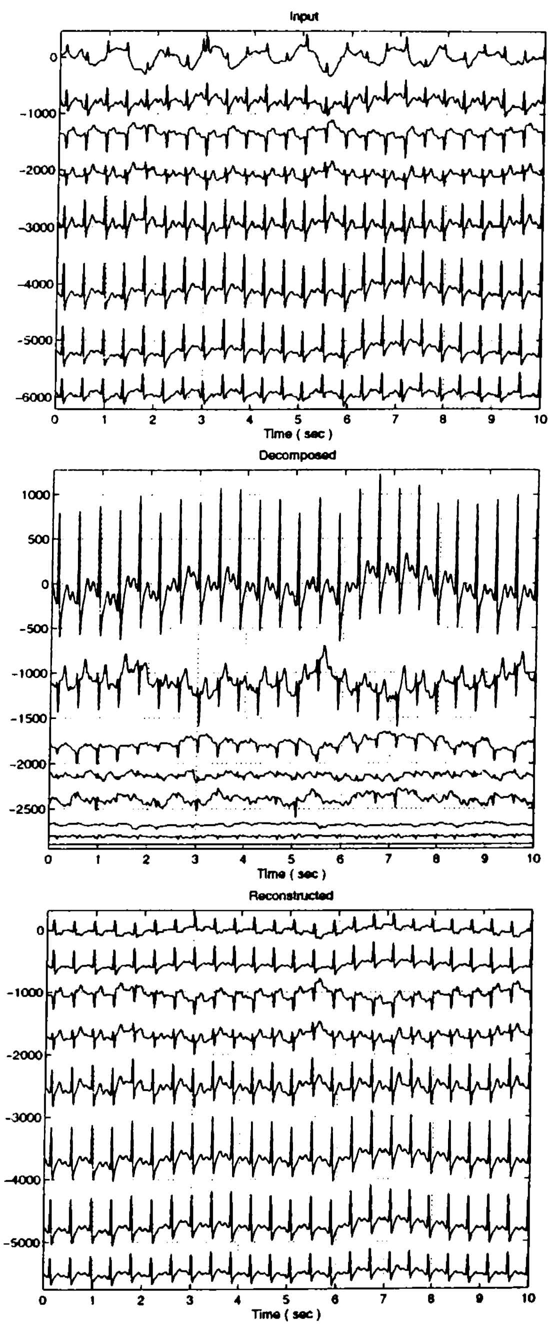

Reconstruction dim.: 2

Excluded channels : 1

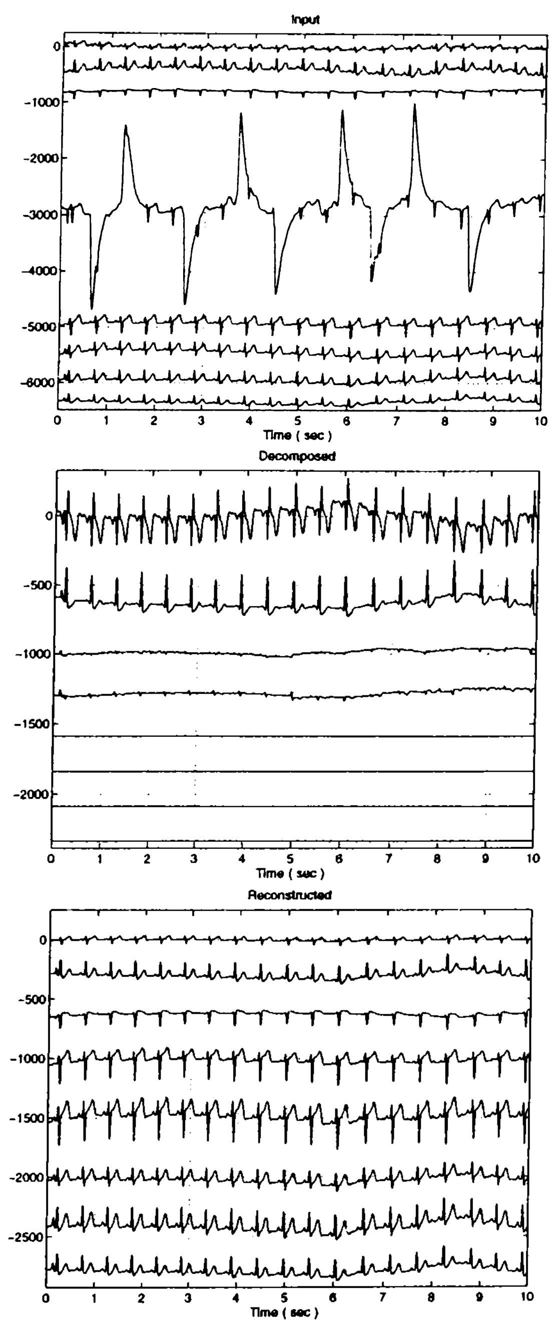

Reconstruction dim.: 2

Excluded channels : 1,2,4,8

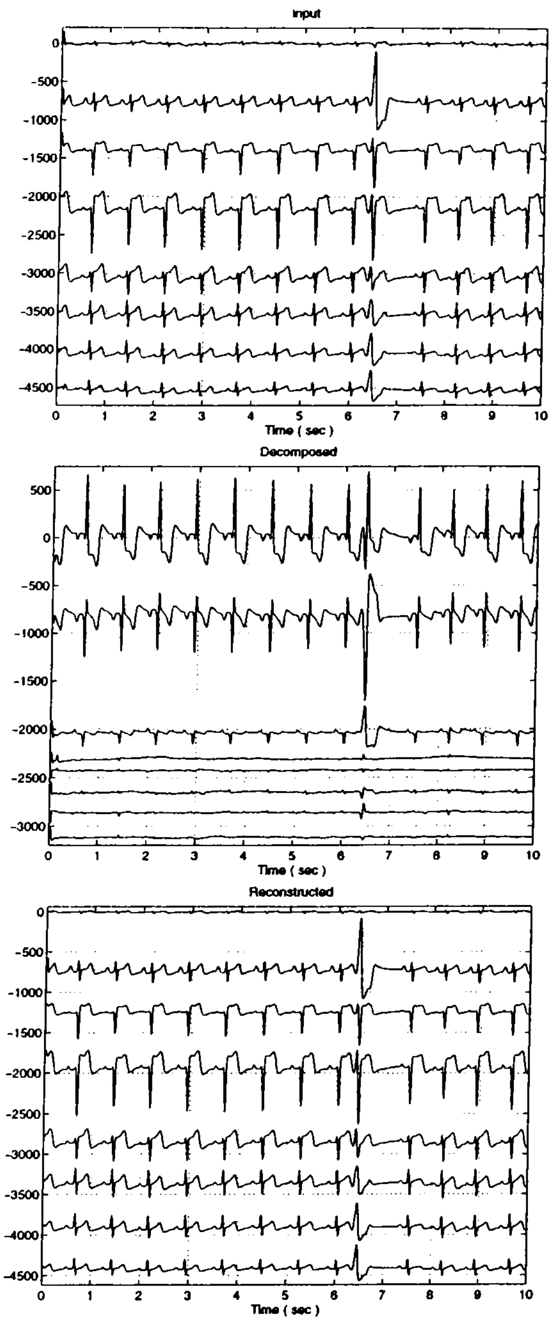

Reconstruction dim.: 3
Excluded channels : No

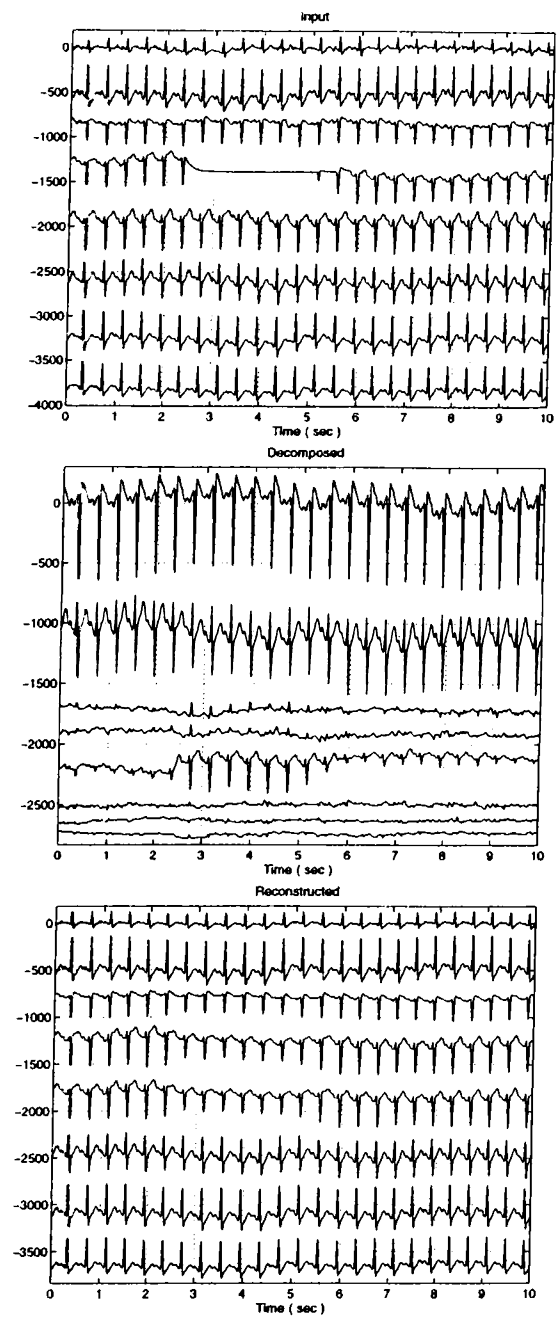

Reconstruction dim.: 2
Excluded channels : No

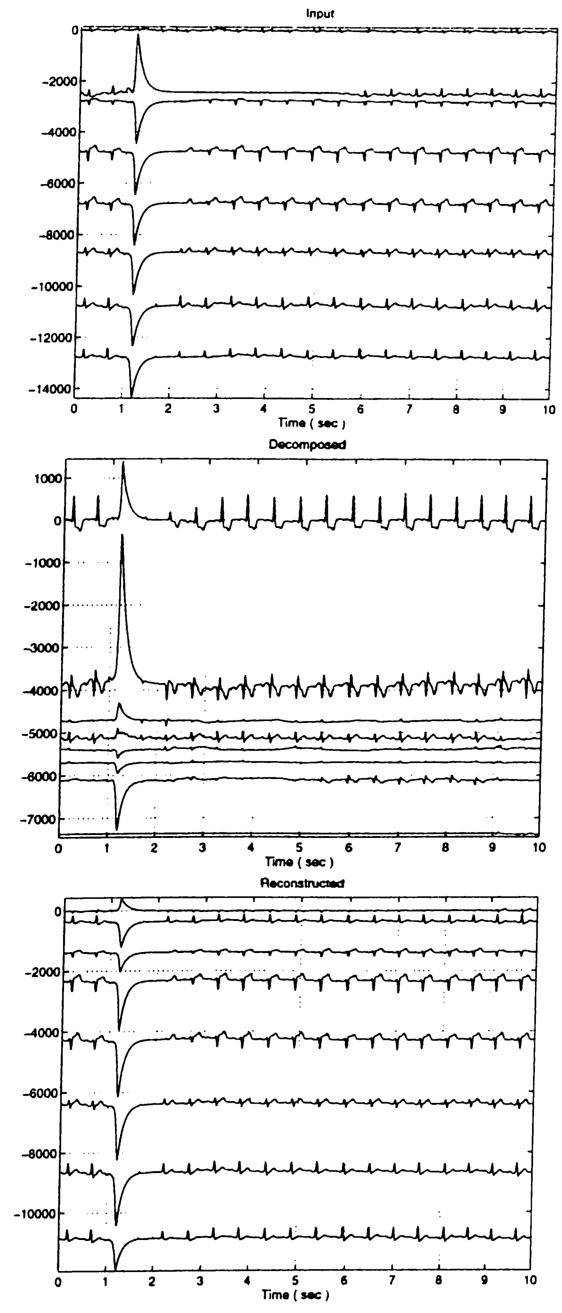

Reconstruction dim.: 2

Excluded channels : 6

Appendix B

High Amplitude, Correlated Noise Case

This appendix demonstrates the performance of the algorithm when high amplitude and correlated noise arrives from the majority of the input channels. No noise detection is applied. The algorithm is capable of separating this noise and keep it in a channel. This channel turns out to the first one because the amplitude of noise is greater than that of the ECG signal. The interesting observation is that the ECG signal is not lost but rather kept in another output channel. The reconstructed signals shown in the figure are reconstructed by using these ECG signal containing channels.

If such a high amplitude and correlated noise can be identified among other noise types, we can continue the reconstruction process without any interrupt.

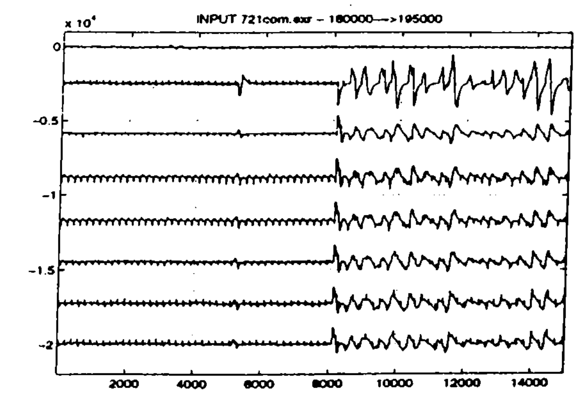
INPUT 721com.exr - 180000--->195000

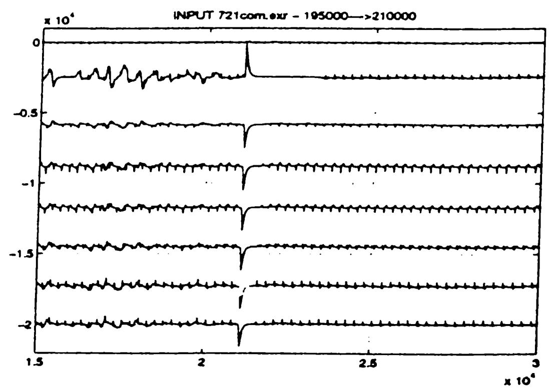
INPUT 721com.exr - 195000--->210000

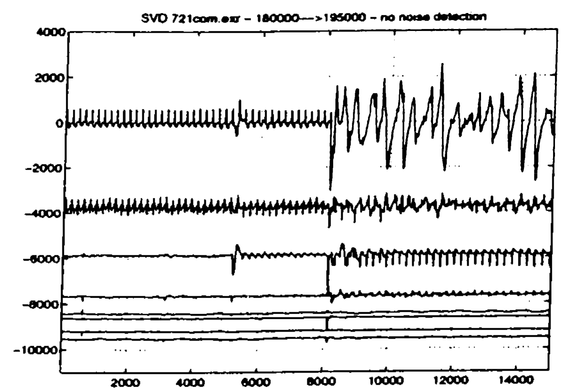
SVD 721com.exr - 180000--->195000 - no noise detection

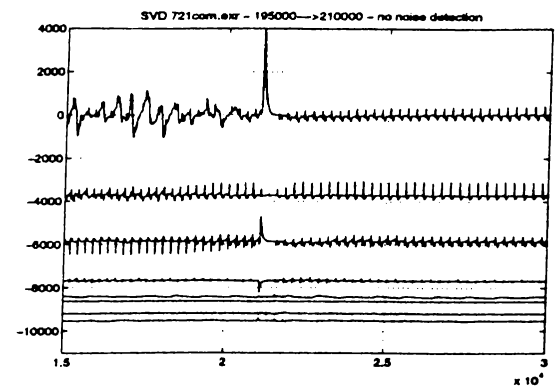
SVD 721com.exr - 195000--->210000 - no noise detection

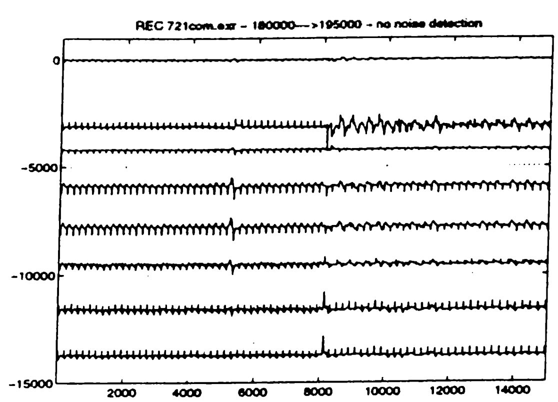
REC 721com.exr - 180000--->195000 - no noise detection

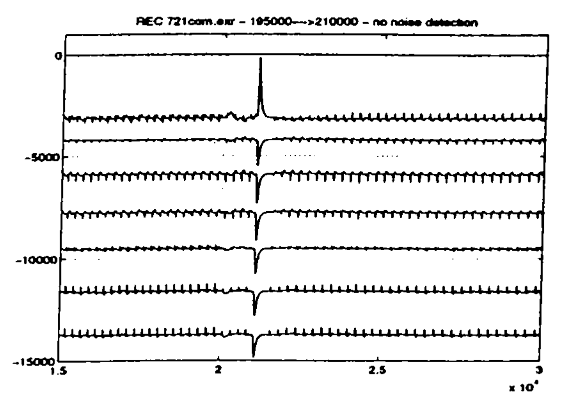
REC 721com.exr - 195000--->210000 - no noise detection

REFERENCES

[1] Sansen W. Vandewalle J. Vantrappen G. Vanderschoot J., Callaerts D. and Janssens J. "Two methods for optimal MECG elimination and FECG detection from skin electrode signals," *IEEE Transactions On Biomedical Engineering*, vol. BME-34, pp. 233–243, 1987.

[2] Muldrow W.K. Moody G.B. and Mark R.G. "A noise stress test for arrhythmia detectors," *Computers in cardiology*, pp. 381–384, 1984.

[3] Mertens J. and Mortara D. "A new algorithm for QRS averaging," *Computers in cardiology*, pp. 367–369, 1984.

[4] Pinto V. "Filters for the reduction of baseline wander and muscle artifact in the ECG," *Journal of electrocardiology*, vol. 25, suppl., pp. 40–48, 1992.

[5] Garson A. Horan L.G. Macfarlane P.W. Mortara D.W. Bailey J.J., Berson A.S. and Zywietz C. "Recommendations for the standardization and specifications in automated electrocardiography: Bandwidth and digital signal processing. A report for health professionals by anad hoc writing group of the committee of electrocardiography and cardiac electrophysiology of the council on clinical cardiology, American Heart Association," *Circulation*, vol. no. 2, pp. 730–739, 1990.

[6] Sornmo L. "Time-varying filtering for removal of baseline wander in exercise ECGs," *Computers in cardiology*, pp. 145–148, 1991.

[7] Mortara D.W. "Source consistency filtering - A new tool for ECG noise reduction," *Computers in cardiology*, pp. 125–128, 1991.

[8] Thakor N.V. Jane R., Laguna P. and Caminal P. "Adaptive baseline wander removal in the ECG: Comparative analysis with cubic spline technique," *Computers in cardiology*, pp. 143–146, 1992.

[9] Nguyen T.Q. Trautmann S. Afonso V.X., Tompkins W.J. and Luo S. "Filter bank-based processing of the stress ECG," *Proc. Annu. Int. Conf. IEEE Eng. Med. Biol. Soc.*, 1995.

[10] Van Loan C. F. Golub G. H. *Matrix Computations.* John Hopkins University Press, Baltimore, 1989.

[11] Per Christian Hansen. *SVD - Theory and applications.* Institute Of Numerical Analysis. The Technical University Of Denmark. Report NI-84-05, 1984.

[12] Anton H. *Elementary Linear Algebra.* John Wiley & Sons, 1987.

[13] Widrow B. and Stearns S.D. *Adaptive Signal Processing.* Englewood Cliffs, N.J. Prentice-Hall, 1985.

[14] Guyton A.C. *Textbook Of Medical Physiology.* W.B. Saunders Company, Philadelphia, London, Toronto, 1971.

[15] Joiner B.L. Ryan B.F. and Ryan T.A. Jr. *Minitab Handbook.* PWS-KENT Publishing Company, Boston, 1985.

[16] Çağlar K. *QRS detection on orthogonalized ECG signals.* Submitted to Bilkent University Eng. Fac. EE Dept. as an MS Thesis, 1996.